Accepted in "Science and Technology of Welding and Joining" – Taylor Francis

Effect of surface oxide layers in Solid-State Welding of Aluminium Alloys - Review

Danka Labus Zlatanovic[1,2], Jean Pierre Bergmann[1], Sebastian Balos[2], Jörg Hildebrand[1], Mirjana Bojanic-Sejat[3*] and Saurav Goel[4,5]

[1]Department of Production Technology, Technische Universität Ilmenau, 98693 Ilmenau, Germany

[2]Department of Production Engineering, Faculty of Technical Science, University of Novi Sad, 21000 Novi Sad, Serbia

[3] Department of Mechanization and Design Engineering, Faculty of Technical Science, University of Novi Sad, 21000 Novi Sad, Serbia

[4]School of Engineering, London South Bank University, London SE1 0AA, UK

[5] Department of Mechanical Engineering, University of Petroleum and Energy Studies, Dehradun, 248007, India

[*]Corresponding author: bojanicm@uns.ac.rs; Tel.+38214852362, Department of Mechanization and Design Engineering, Faculty of Technical Science, University of Novi Sad, 21000 Novi Sad, Serbia

Abstract

This review sheds novel insights on the residual oxide behaviour of solid-state weld joints of aluminium alloys. Understanding the influence of oxides on the aluminium surface before and during welding, its impact on the weld structure and possible solutions for reducing its impact were addressed. The solid-state techniques most relevant to the transportation sector namely, diffusion bonding, friction stir spot welding and ultrasonic welding were surveyed, analysed and reviewed. During this analysis, the implication of the presence of oxides on aluminium substrate affecting the metallurgical characteristics of the weld joints were reviewed. Visible defects such as voids, delamination, kissing bond, and hook defects, and problems associated with these defects were analysed and few suggestions are made to partially overcome these issues.

Keywords: Residual oxide; Aluminium alloy; Friction stir spot welding; Diffusion bonding, Ultrasonic welding

Contents

Abbreviations**:**

AS	Advancing side
CDRX	Continuous dynamic recrystallization
CFSSW	Conventional friction stir spot welding
DB	Diffusion bonding
EDS	Energy-dispersive spectroscopy
e-TEM	Environmental transmission electron microscopy
FSW	Friction stir welding
FFSSW	Flat friction stir spot welding
FSSW	Friction stir spot welding
IPDB	Impulse pressuring diffusion bonding
IPADB	Impulse pressure-assisted diffusion bonding
PLT-FSSW	Pinless tool friction stir spot welding
PFSSW	Protrusion friction stir spot welding

RFSSW	Refill friction stir spot welding
RS	Retreating side
RZ	Recrystallized zone
SEM	Scanning electron microscopy
TEM	Transmission electron microscopy
TWI	The Welding Institute
USW	Ultrasonic welding
WFI	Weld faying interface
WFSSW	Walking friction stir spot welding
XPS	X-Ray Photoelectron Spectroscopy

Nomenclature**:**

A_c	The area of contact
A_n	Fraction of normal area
Tm	Melting point
Y	Flow stress
σ_{eff}	Local effective von Misses stress
σ_n	Normal contact stress
τ_{app}	Normal shear stress

1. Introduction

Over the years, various solid-state welding techniques have evolved to joining aluminium alloys which rivals fusion welding techniques. Solid-state welding gained prominence due to its cost-effectiveness and lower consumption of energy [1,2]. Furthermore, due to low process temperature, the propensity of heat-induced defects such as pores, hot cracks, slag inclusions, brittle solidification, or high distortion due to residual stresses during solid-state welding are suppressed [3].

Despite various advantages, solid-state welding techniques have yet to realise their full potential. One of the problems for instance during solid-state welding of aluminium arises from the oxide layer present on the aluminium surfaces before the welding [4,5]. Atmospheric oxygen reacting with the aluminium surface creates a barrier for the heat to diffuse uniformly in the stir zone, which affects the homogeneity of the weld joint resulting in the reduction of mechanical and electrical properties of the component, especially at the interface. It can mathematically be explained by the fact that the process temperatures during solid-state welding of aluminium range from 0.4 to 0.8 of its melting point. As opposed to aluminium, which melts at about 660°C, the aluminium oxide layer has a melting point of 2072°C. Thus, the process temperature during solid-state welding of aluminium does not melt or even sufficiently soften the oxide layer. The partially interrupted oxide fragments become interspersed and remain entrapped in the weld faying interface leading to the formation of residual oxide defects causing problems such as delamination, and compromised properties such as reduced shear, bending and fatigue strength [5–7].

According to solid-state welding theory, the joining process will achieve superior results if the two metal parts to be welded together are free from oxides and surface contaminations prior to the welding [8,9]. To overcome the obstacles arising from the oxide layer or other surface contaminants, the solid-state joining process utilises the combined influence of heat (below the melting point), and pressure during the dwell time [10]. The initial contact between the two asperities during solid-state welding introduces a series of voids which could subsequently act as nucleation sites to fracture [11]. Thus, void shrinkage is an important consideration in obtaining high-quality solid-state weld joints. These

voids have been attributed to physical mechanisms [11,12] such as side flow of the surrounding material (plastic deformation and creep deformation) and atomic diffusion between various surfaces (surface, interface and volume diffusion). An increase in temperature reduces yield strength and facilitates plastic flow. When complemented by pressure it draws the material from adjacent regions into voids. This is accelerated further by the accelerated atomic diffusion [9].

Some solid-state welding techniques prove to be quite effective for welding dissimilar metals that are difficult to weld with conventional welding techniques due to the metallurgical incompatibilities. The major disadvantage of solid-state welding is that it needs expensive equipment and substantial sample preparation which increases processing time [10]. Furthermore, additional limiting factors can influence the applications such as the joint design, the limited thickness of the workpieces, or the need for a vacuum chamber. Most of these problems can be overcome by reducing or eliminating the influence of the oxide layer on the diffusion process during solid-state welding. However, despite all research done in this field, the problem is still not resolved completely. Up until now, the problem of entrapped oxides has not been eradicated and instead researchers have just been trying to find a favourable window of processing using trial-and-error approaches using parametric optimisation.

Although significant efforts have been made in the past to understand the physical and metallurgical behaviour of residual oxide defects, the research on this topic is still in its infancy and more efforts are required to address this problem systematically. In the next section, an attempt is made to connect the theoretical background and experimental experience obtained during various solid-state technologies. This background highlights the exact problem due to the residual oxide layer during solid-state welding of aluminium. Furthermore, the interrelated solid-state techniques such as diffusion bonding (DB), friction stir welding (FSW) and ultrasonic welding (USW) used to join aluminium alloys were studied to establish common problems these methods have. 0

2. Background of Solid-State Welding

According to the most widespread welding theory, all metals should spontaneously bond together if the atoms are brought to a close interatomic distance., Also, the necessary attraction force between the

ions and the electrons is reached when the interatomic spacing is less than 2.86 Å [13]. The attractive force will form a joint, while the crystal mismatch causes a non-cohesive grain boundary [10,14]. Thus, bonded surfaces would have to be perfectly smooth and clean. However, in practice, this is hard to achieve because bonded sheets will have surface roughness much higher than 2.86 Å. Even after polishing microscopic surface roughness exist. There is also a problem that the oxide layer quickly develops on top of most metals, especially aluminium. The oxide layer (particularly the amorphous layer) acts as a barrier for two atoms from different sheets to form an attractive bond. Furthermore, some other contaminants such as oil, moisture, gas, corrosion, and absorbed water vapour can also be present on the metal surface. Even in traces, they represent a strong barrier to the atomic bonding. Therefore, to obtain an atomic bond between two metals without melting, these barriers must be overcome. Overcoming these barriers is the biggest challenge for all solid-state welding processes. Most solid-state welding processes use elevated pressure and temperature or involve a high level of deformation [15] or vibration assistance [16–18]. Sometimes, if it is necessary, contamination, water vapour and oxides can be reduced or completely removed by using chemical surface treatments [19], special protecting gases [20] or special techniques [21], however those processes are either expensive or require additional time which reduces the yield. Several mechanisms are postulated over the years to describe the bonding during the solid-state welding processes. These theories are discussed below.

2.1. Film theory

The film theory was proposed to explain the low-temperature solid-state welding process. To achieve a stable bond between the two sheets, intimate contact between the metal surfaces is required. The clean metal surface can be obtained by stretching the bond line and fragmenting the oxide layer causing diffusion to occur between the oxide fragments. This way, the underlying material between the oxide’s fragments become exposed and because of the high pressure, it gets extruded through the cracks. The presence of different surface oxides and contaminants is responsible for variation in the mechanical properties of solid-state welded metals [4,22,23]. Therefore, if the oxide layer is present on the surface to achieve bonding between two metals it is necessary: (i) to expose substrate metal by

fragmenting or removing the oxide film and (ii) to provide axial load which will establish close contact between the substrate metal [14].

Pilling [24] and Hill et al. [11] proposed the model for diffusion bonding suggesting that the mechanisms operating during DB are based on those derived from pressure sintering studies. It was proposed that at the interfacial free energy reduction is similar to the sintering process and the applied joining pressure causes the closure of gaps, while the kinetics is governed by the interfacial mass transport at elevated temperatures [24,25]. Accordingly, Cooper et al. [26] proposed an improved film theory. As solid-state bonding occurs at temperature of about 0.8 times of the melting point of the material, the diffusivity also enhances. It is generally known that aluminium and its oxides are insoluble at low temperatures, so diffusion will act to increase the area of substrate contact between islands of fragmented oxides, rather than replacing the film theory mechanism shown in Figure 1.

Rahaman [27] proposed the model to explain the mechanism of solid-state sintering, while Cooper et al. [26] proposed a modified theory to explain the diffusion bonding between the oxide fragments. The mechanisms relevant here are: (a) Grain boundary diffusion, (b) lattice diffusion from the grain boundary to the neck, (c) plastic flow and (d) lattice diffusion from the particle surfaces cause neck growth and push the oxide and other impurities from the neck. Grain boundary and lattice diffusion are dominant mechanisms during diffusion bonding between the metals. The role of plastic flow followed by dislocation accumulation of metals is controversial.

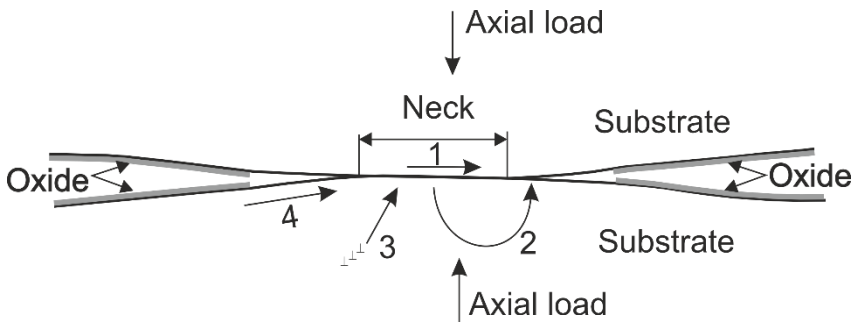

Figure 1. Schematic of the diffusion mechanisms causing an increase of contact area between two substrates: Mechanisms:1-Grain boundary diffusion, 2-Lattice diffusion (from the grain boundary), 3-Plastic flow, 4-Lattice diffusion (from the surface) (adapted from [26,27]).

2.2. Energy barrier theory

2.2.1 Mismatch of the crystal lattice theory

The mismatch of the crystal lattice theory was originally proposed by Semenov et al. [28]. To obtain the bonding between two metals using solid-state technique, it is necessary to have distortion of the crystal lattices of the two surfaces by overcoming a certain energy barrier. This theory was challenged by the work of other researchers who proved that bonding can proceed without deformation (energy-free bonding) if there are no barriers between the two surfaces [29].

2.2.2 Recrystallisation theory

Recrystallization theory proposes that crystal growth during recrystallization eliminates non-metallic barriers [30]. Several researchers have attempted to explain the recrystallization mechanism during solid-state welding which includes severe plastic deformation. Andalib et al. [31] observed dynamic recrystallization as a refining grain mechanism during friction stir spot welding of $AlMg_3$ aluminium alloys. Also, the dynamic recovery causes the formation of highly refined and equiaxed grains. Jata et el. [32] proposed continuous dynamic recrystallization (CDRX) as a mechanism responsible for weld formation. During FSW/FSSW the friction-induced temperature, strain and strain rate, as well as a complex interaction between dislocations and solute atoms cause CDRX to occur.

Several researchers concluded empirically that during FSW, an increase in applied stress (axial and shear) and process temperature enhances the degree of bonding. However, it does not change significantly with the increase of clamping force (which holds two pieces together). This indicated that creep has a more critical role during FSW than diffusion on bond evolution. Labus Zlatanovic et al. [33] pointed out that the axial and shear load/stresses have the highest influence on weld properties. The proper combination of these two parameters led to the bonding of four sheets even though the tool penetrated only the first (top-most) sheet. A combination of film and recrystallization theory was used to explain the bonding during friction stir spot welding with the pin-less tool. Sharma et al. [34] indicated that the joint strength depends on the shear ratio driven by the rotational speed, while it was not significantly affected by the processing time.

Several researchers [35–37] have supported those theories. However, these are applicable to weld formation only during high deformation processes such as FSW. During diffusion bonding or ultrasonic welding, this phenomenon does not persist due to low (micro) level of deformation.

Ultrasonic welding has paved way to the formulation of various theories, which are generally divided into three main directions: The first direction considers diffusion processes as the main mechanism of bonding. Sriraman et al. [38] and Mariani et al. [39] both proposed dynamic recrystallisation and grain boundary migration as a bonding mechanism during USW. Gunduz et al. [40] considered that these diffusion processes are accelerated by a high instantaneous vacancy concentration generated by high strain rate plastic deformation. Another USW theory considers that for strong bonding, localised melting of the weld interface is required [40,41]. However, a vast majority of the USW studies have proved that the interfacial melting is not required to obtain strong bonding. A well-established theory of USW has been attributed to the bonding due to the heat-induced plastic deformation of the surface asperities at the weld interface. The local plastic deformation creates clean metallic junctions and brings faying surfaces into close contact [42]. It is considered that flow stress of the surface asperities decreases during the bonding. There are two main hypotheses, which describe softening mechanisms. One of them is proposed by Kelly et al. [43] and considers acoustic softening as a main softening mechanism while thermal softening is found to be relatively minor (less than 5% of total softening). The acoustic softening results from the interaction between acoustic waves and dislocations of metal grains (ultrasonic-induced dynamic recovery) [44]. However, several researchers have suggested that acoustic softening in some papers was misinterpreted as thermal softening caused by frictional heating at the bonding interface [42,45]. This mechanism is widely accepted, but its role was differently interpreted by different researchers [42,43]. According to most relevant research during the solid-state welding process, the combination of more than one theory governs the charactersticsof the weld formation.

3. Aluminium alloys and growth of surface oxide film

3.1 Aluminium alloys

Aluminium is one of the most commonly used metals, with annual consumption of about 35 million tonnes [46]. Its suitable mechanical properties, conductivity, barrier properties, corrosion resistance and low mass density are the main reasons for continuous use in many sectors. Particularly, the lightweightness of aluminium and its alloys is highly attractive to the electronics, transportation and aerospace sectors [47].

As such in the annealed condition, pure aluminium has a low yield strength of about 7 to 11 MPa. To improve on this aspect, alloying of aluminium was explored for enrichment and enhancement of its properties. Even though aluminium can be alloyed with most alloying elements, selective metal offers appropriate alloying more than 10% atomic weight which are Zn, Mg, Cu and Si. Mg and Cu are among the most effective strengthening elements (at 0.5 % or less) [48,49].

Aluminium possesses high stacking fault energy (~170 $mJ \cdot m^{-2}$). During deformation, the cellular substructure can form inside the grains rather than stacking faults or twins. Cellular substructure causes strengthening [30,50].

At low processing temperatures, the substructure formed by work hardening is referred as the cells-structure. Those cells differ in orientation by about 1° and have walls comprising of tangled dislocations. However, subgrains formed by deformation at higher processing temperatures are bound by well-defined, narrow walls. Their misorientation is higher compared to that of the cells (up to 15°). During the recovery process, the value of m changes from 1 to 0.5, which causes the substructure to transform from cells to subgrains. This transformation causes improvement in the mechanical properties.

Age-hardened alloys decreases solid solubility of one or more elements at low temperatures. Most ageing alloys will undergo some hardening effect at room temperature (natural ageing) and it can last indefinitely with a drop in the ageing rate over time. On the contrary, artificial ageing takes place at elevated temperatures and hardness usually increases to the maximum value and then decreases

(overaging). When a critical dispersion of intermediate precipitates is present, the maximal hardness is obtained [51].

3.2 Growth of oxide film on aluminium surfaces

Over the years, several studies have been performed to understand the behaviour of self-forming aluminium oxide on aluminium surfaces. Those studies were mostly performed on bare aluminium surfaces through oxidation [30,35,52,53]. The development of oxide film on the aluminium surface in the presence of atmospheric oxygen involves absorption and dissociation of oxygen on a bare aluminium surface, oxide nucleation, and oxide-film growth. When the entire surface of aluminium is already covered by an oxide film, further growth is restricted by the transport of the reactant type through the oxide film [54–56]. Studies have shown that the composition and the structure of growing oxide film vary depending on the oxidation temperature, time and oxide thickness.

Snijders et al. [57] studied the growth of aluminium-oxide films by dry, thermal oxidation of a bare Al (4 3 1) substrate in the temperature range from 100 to 500 ˚C at a partial oxygen pressure of 1.33×10^{-4} Pa. The development of aluminium oxide film structure as a function of time, temperature and oxide thickness from the relative contribution of the amorphous and crystalline γ-Al_2O_3 basic spectra to the resolved oxide film upper valence band (UVB) spectra were studied. It was established that with the increasing temperature and thickness of aluminium oxide film up to 1 nm, the nature of the oxide film is highly amorphous and the oxide layer above this thickness was mostly crystalline. Jeurgens et al. [54] confirmed these results using X-Ray Photoelectron Spectroscopy (XPS). Kinetic analysis proved the existence of two different oxide film growth regimes. The first one was the initial regime of the fast growth of amorphous uniform limiting oxide film and the second, slower oxidation regime was observed only above 300˚C where initially grew aluminium enriched amorphous oxide film attains stoichiometric composition of Al_2O_3. and becomes crystalline γ- Al_2O_3. eventually.

Jeurgens et al. [55] developed a model to test the thermodynamic stability of a thin amorphous metal-oxide film on top of a single-crystal metal substrate as a function of temperature, film thickness and crystallographic orientation of the substrate. Studies showed that for a certain thickness of oxide films,

the amorphous state was preferred over the crystalline state. The higher bulk energy of the amorphous film as compared to the crystalline oxide film can be overcompensated with the relatively low sum of amorphous oxide surface energy and crystalline metal – amorphous oxide interfacial energy. The critical thickness up to which the amorphous oxide film is thermodynamically more stable than that of the corresponding crystalline oxide can be calculated by the total energy of the metal-substrate metal-oxide film system i.e., including Gibbs energy of formation, mismatch energy and interfacial and surface energies.

Nguyen et al. [58] were the first to study full oxide growth regime from the oxide nucleation to complete saturated, few nanometres-thick surface film with help of atomic resolution imaging in an environmental transmission electron microscope (e-TEM).

Figure 2 show key steps during the oxidation of a (100) surface facet at an oxidation pressure of 3×10^{-5} Pa. In Figure 2a, an early stage of oxidation through the nucleation of oxide islands at the atomic terraces on the surface can be seen. Thereafter oxide islands grew laterally towards one another as shown in Figure 2b,c. After a sufficient time (Figure 2d), the surface becomes covered with a continuous semicrystalline layer of oxide approximately 1.5 nm thick. The fully thickened film consists of the expected amorphous oxide structure. Those results were in good agreement with surface science measurements of the early stage of oxidation and average data obtained from the bulk techniques.

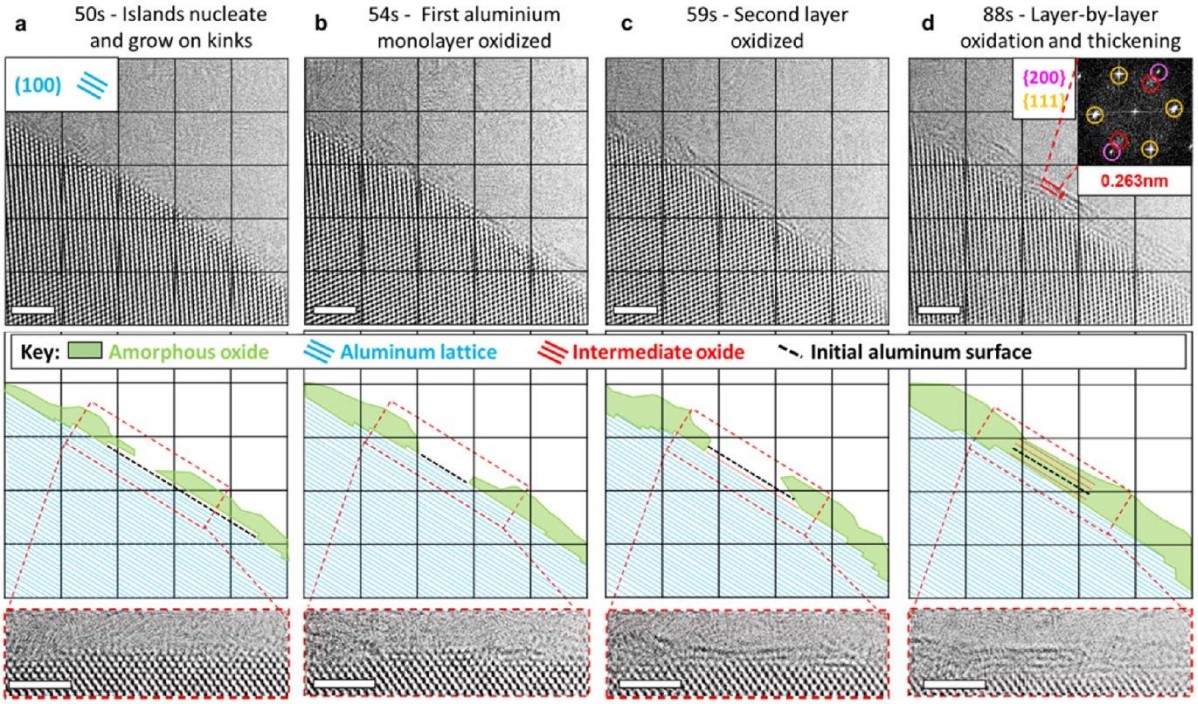

Figure 2. Top: (a-d) Time-resolved e-TEM images showing growth of aluminium oxide over the oxidation time; Bottom: schematic illustrations of the structures visible in the top TEM images, with an enlarged TEM image of the surface region shown below [58].

A previously mentioned studies [54–58] refer to the ideal state when the oxides grow unhindered on a clean aluminium substrate. However, most aluminium foils, sheets and plates used in welding processes are subjected to metalworking processes such as hot/cold rolling, grinding, milling or/and machining. The interaction between the tool and the substrate surface can cause metal transfer from the workpiece to the tool. This transfer can initiate through different mechanisms such as micro-cutting, adhesion, delamination, etc. The transferred metal oxidizes and retransfers back to the surface which adversely influence the properties of the surface. The most influenced properties are surface appearance, formability, weldability, etc.

The subsurface of metals subjected to sliding (as such between the tool and workpiece) were studied a long ago which is commonly referred to as Beilby layer. Beilby [59] made a detailed microscopic study of the effect of polishing on a wide range of materials. He concluded that the polishing process resulted from the flow of material caused by the local melting of asperities resulting in an amorphous

layer. Beilby’s first hypothesis was widely accepted [60]. However, in 1982 Samuels [61] proposed that the amorphous surface layer was the result of the micro-cutting process and local microplastic deformation rather than the flow of liquid metal over the surfaces. A detailed study of Beilby layers on worked aluminium alloy began in mid-1990s with the seminal work of Leth-Olsen [62]. The study revealed that the Beilby layer formed on hot and cold rolled AA 8006 and AA 3005 aluminium alloy sheets were between 0.4 and 0.8 μm thick and compressed from ultrafine grains. This study together with that of Fishkis et al. [63] study initiated a series of TEM studies on deformed surface layers of a wide range of aluminium alloys subjected to hot and cold rolling, grinding, machining and mechanical polishing. Scamans et al. [64] gave a detailed overview of these studies. They showed that the layers were microcrystalline rather than amorphous, and they strongly govern the corrosion resistance and reflectance.

All these studies were performed under non-metalworking conditions. Fishkis et al. [63] were the first to study the surface behaviour of aluminium-magnesium alloy subjected to metalworking condition during hot rolling. Their results revealed that the surface layer was composed of ultrafine grains of 40 to 200 nm diameter that were Zener pinned by fine magnesium oxide particles of 25 Å (Figure 3). This layer consists of a transition mixed substrate film 1.5 to 8 μm thick and continuous oxide film (250 to 1600 Å). The transition film was placed between the surface layer and the underlying bulk alloy. The composition of the continuous oxide film was found to be MgO. After the first and second passes of hot rolling, the mixed substrate was found to consist of a mixture of MgO, γ-Al_2O_3, and spinel $MgAl_2O_4$. Furthermore, after the third and fourth passes, the embedded crystalline oxides contained mainly MgO and γ-Al_2O_3, and after the sixth pass, there was only MgO.

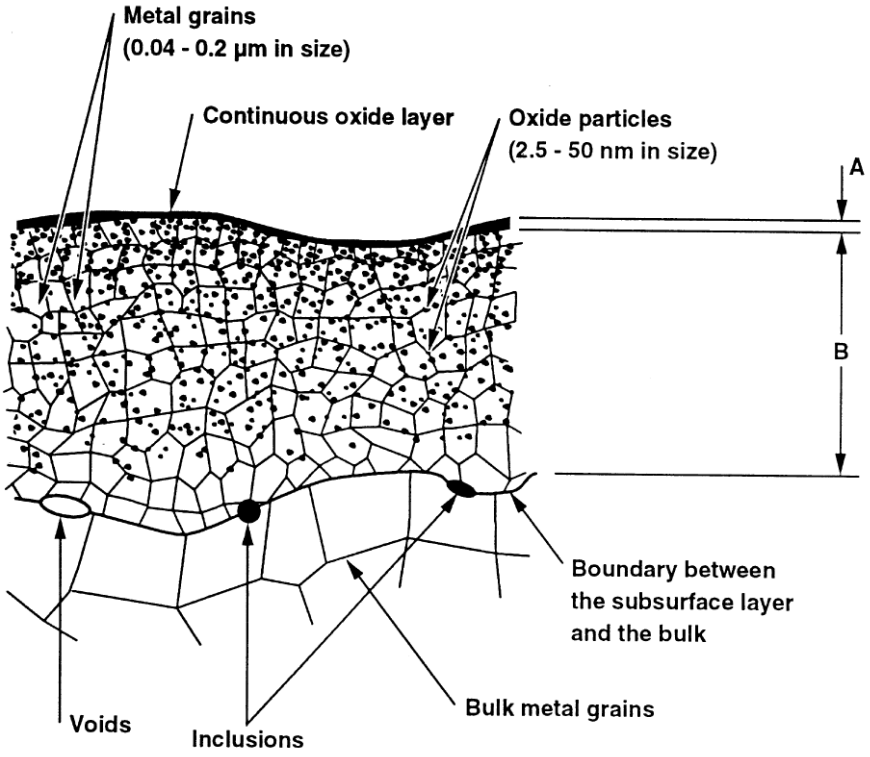

Figure 3. Schematic of the subsurface film containing microcrystalline oxides mixed with fine-grained metal structure and covered with continuous oxide film; (A) thickness of continuous oxide film (250 to1600 Å); (B) thickness of mixed substrate film (1.5 to 8 μm) [63].

4. Diffusion bonding

4.1 Basic principle

Diffusion bonding is a solid-state welding process where bonding occurs through the interdiffusion of elements between two workpieces, with carefully cleaned surfaces, at high pressure and elevated temperature. The temperature is usually in the range of $(0.5\text{-}0.8)\cdot T_m$ where T_m is the melting point of the material [8]. The interfacial pressure is low enough to prevent large-scale deformation although local deformation at the interface can be substantial. Since diffusion bonding is a result of the mutual diffusion of atoms at the interface, bonded surfaces are required to be cleaned to prevent oxide contamination. Therefore, the process is performed in vacuum [65] or in a protective atmosphere [66].

During diffusion bonding, the workpieces are heated in a furnace at a high temperature to perform the joining process. Workpieces are placed in a vacuum chamber or in a chamber filled with inert gas, between the two rods such that the top is loaded with a predefined axial load. Suitable bonding temperature, bearing pressure, bonding time and environmental conditions (vacuum or inert gas) lead to strong bonding.

Diffusion bonding (DB) is mostly used in the aerospace industry, electronics, and nuclear applications. The most significant advantage of the DB process is high-quality weld without pores, inclusion, and chemical segregation. Furthermore, there is no limitation on the workpiece thickness. However, DB process is time-consuming with low productivity and requires time and money for surface preparation [67].

4.2 Models proposed for diffusion bonding of aluminium

To obtain good quality diffusion bonding between two aluminium workpiece surfaces using diffusion bonding, a few obstacles need to be overcome:

(i) to interrupt the oxide layer between the sheets;

(ii) to establish close contact between two surfaces and

(iii) to press the two sheets, close enough so extrusion of clean metal occurs.

4.3 Establishing close contact

When two rough surfaces are pressed together, the initial contact is only made between asperity tips. In that case, the area of contact (A_c), as a fraction of the normal area (A_n), is equal to the normal contact stress (σ_n) divided by the aluminium flow stress (Y). However, Conrad et al. [68] found that the true area of contact is about 80% of this ratio. This difference is caused by a tri-axial stress state in materials surrounded by asperities, constraining plastic flow. Therefore, the true contact area for modelling is presented by equation (2) [14]:

$$A_c = 0.8 \cdot \frac{\sigma_n}{Y} \cdot A_n \qquad (2)$$

If A_c is higher than A_n, A_c should be equal to A_n.

If the normal shear stress τ_{app} is applied as an addition to normal contact stress σ_n, local effective von Mises stress will be (σ_{eff}) equation (3) [14]:

$$(\sigma_{eff})^2 = \left(\frac{\sigma_n \cdot A_n}{A_c}\right)^2 + 3 \cdot \left(\frac{\tau_{app} \cdot A_n}{A_c}\right)^2 \quad (3)$$

To maintain local equilibrium $(\sigma_{eff} = Y)$, the area of contact must increase to:

$$A_c = 0.8 \cdot \frac{\sqrt{\sigma_n + 3 \cdot (\tau_{app})}}{Y} \cdot A_n \quad (4)$$

The parameter Y (flow stress) is the function of strain, strain rate and temperature [14,69]. However, during the diffusion bonding of aluminium sheets, initial contact will occur between the oxide films. Since aluminium has chemically stable oxide film, which is not insoluble at diffusion bonding temperature, diffusion cannot occur unless the oxide film is removed or fragmented.

4.4 Approaches to interrupt the oxide layer at the weld interface during diffusion bonding

According to Shizardi [70], there are a few different approaches proposed to disrupt the oxide layers to ensure good-quality diffusion bonding which are explained further sequentially:

(i) Imposing substantial plastic deformation or enhancing microplastic deformation of the surface asperities

(ii) Use of interlayers and the effect of alloying elements.

(iii) Use of impulse pressure.

(i) Imposing substantial plastic deformation or enhancing microplastic deformation of the surface asperities

During solid-state diffusion bonding of aluminium and alloys, the continuous brittle oxide film can be fragmented by imposing substantial plastic deformation. Considering that the oxide film has significantly lower ductility than the pristine metal, it ruptures when subjected to high plastic deformation. As shown in Figure 4 metal to metal contact is promoted because of the local breaking of the brittle oxide film after contacting the asperity tips. Urena et al. [71] showed that about 40%

deformation was required to obtain quality bonds by welding discontinuously reinforced SiC/Al matrix composite foils from aluminium-copper alloy.

Although some researchers have obtained high-strength joints by applying substantial plastic deformation during diffusion bonding, this approach has limited applications due to a need for significant plastic deformation of the pristine metal.

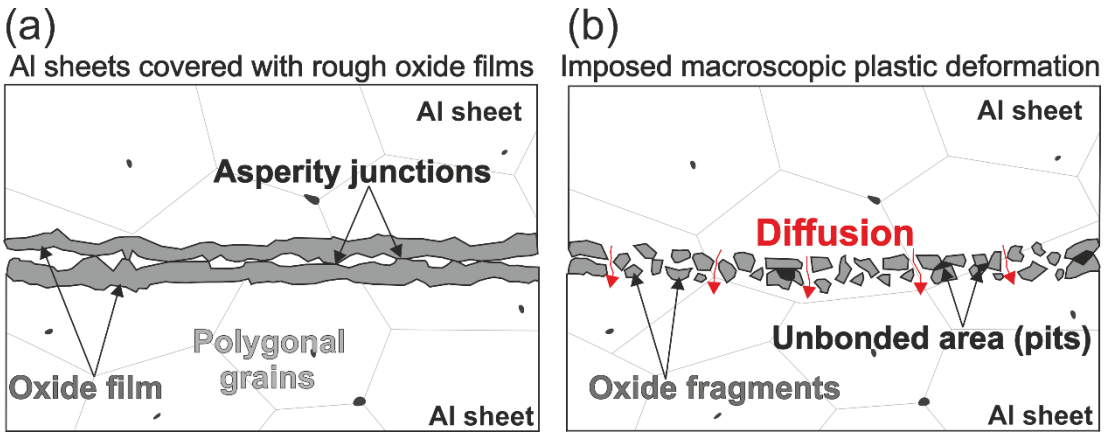

Figure 4. (a) Two aluminium sheets with interfacial thin oxide layer: (b) interrupted oxide layer by imposing plastic deformation (adapted from [4]).

An alternative approach for enhancing macroscopic plastic deformation is to use a fairly rough surface finish, which can lead to higher bond strength than a polished surface finish. Rough surfaces cause a higher level of plastic deformation imposed on the asperities, which induces more oxide fragmentation. Therefore, metal-to-metal bonding gets enhanced. It was suggested that the local plastic deformation in the initial stage ruptures brittle oxide asperities, which leads to improved metallic contact between the workpieces. The rougher the surface, the higher the level of the plastic deformation implemented on the asperities, which leads to more oxide fracture and consequently metal-to-metal bonding enhancement [8,70].

Tensi et al. [72] reported some effects of different surface preparation methods on the bond quality of DB high-strength aluminium sheets. The experimental results confirmed that increasing the local deformation by increasing the surface roughness leads to higher bond strength. Brushed surfaces lead to quality bonds due to a high recrystallization effect and enhanced interfacial diffusion by an

increased dislocation density. However, Zhu et al. [73] reported opposite results after DB of high niobium containing Ti-Al alloy. It was reported that with a higher level of roughness, white layer α_2 (Ti_3Al) appears, which decreases the shear strength of bonds. It was also reported that with a high roughness level, a higher amount of air is entrapped between asperity tips, which enhances white layer formation. This inconsistency regarding the effect of surface roughness on weld strength is probably due to the different properties and chemical composition of the studied materials. Shear testing at toom temperature revealed that high-energy shot peening was beneficial to lower the bonding temperature and ensure a joint shear strength of 420 MPa.

(ii) Use of interlayers and effect of alloying elements

One of the first research on diffusion bonding with interlayers was performed in 1964 by Barta [74]. The paper reported low-temperature diffusion bonding of Al-7075 with various interlayers: silver, gold, nickel, aluminium, tin, zinc, iron, copper and magnesium. The interlayers were electroplated, vacuum deposited, plasma-sprayed, loose foils and clad Al-7072. A low bonding temperature (150-230 $^{\circ}$C) was used in combination with high pressure of 165 MPa. Investigations with most of the interlayers resulted in either no bonds or very poor bonds. However, over the years, diffusion bonding with interlayers has significantly improved. The interaction between the interlayers and pristine material is a very complex process and sometimes contradicting. It depends on many factors such as purity, surface roughness and chemical composition of all materials involved, method of deposition and thickness of interlayer. The relative thickness and ductile properties of the interlayer material influence the stress-strain state at the bond interface and the contact effect such as hardening/softening [75]. Depending on the type of material used for bonding, interlayers can be classified by their purpose:

- Interlayers for reducing bonding pressure and temperature [76];
- Superplastic interlayers are used for preventing plastic deformation of pristine material at weld faying interface [77];
- Interlayers for removing or preventing the formation of oxide layers during bonding [78];

- Transition liquid phase diffusion bonding – molten interlayers for producing high-strength precision joints by the formation of liquid phase at weld faying interface [79,80].

The interlayers have a role in all bonding stages during diffusion bonding. During physical contact formation, the proper selection of the interlayer greatly reduces or prevents residual macroplastic deformation of the parent metal in the joints by deforming the interlayer instead. To bond the materials with higher hardness and brittleness, it is necessary to use interlayer activators of the bonded surfaces, which have higher ductility compared to those of parent metal. Depending on the interlayers’ purpose, they are implemented in the form of foils, films and coatings, deposited on one or both bonding surfaces by electroplating or vacuum spraying, rolling of powders or combining the spraying and foil [75].

Habisch et al. [81] obtained a high-strength bond between dissimilar metals: aluminium alloys (AA 6082, AA 7020 and AA 7075) and magnesium alloy (AZ 31 B) by using silver and titanium interlayers. Titanium interlayer produced joints with higher strength (from 35 to 50 MPa for different aluminium alloys) compared to those produced with a silver interlayer (from 20 to 28 MPa for different aluminium alloys). The reason being the silver interlayer which completely diffuses into pristine materials and forms a brittle diffusion zone, which decreases the weld strength significantly. Dunford et al. [82] used copper interlayers during diffusion bonding of AA 8090. Transient liquid phase formation and melt solidification were controlled by solid-state diffusion of copper along the Al-Li alloy grain boundaries. The main bonding mechanism was enhanced copper diffusion along the grain boundaries and in the liquid phase. The joint shear strength was greater than 90%. of base material strength. The best result was obtained with an interlayer thickness of 6 μm when shear strength was 224 MPa while base metal had a strength of 226 MPa. Nami et al. [83] used copper interlayer for diffusion bonding of Al/Mg_2Si metal matrix composite. It was reported that with the use of the copper interlayer, less deformation can be achieved with the same shear strength. The strength of the weld joints was better compared to no interlayer for the same welding conditions used. Wu et al. [84] also reported diffusion bonding of another aluminium-lithium alloy (AA 1420) but with an interlayer made of pure aluminium. It was reported that when a pure aluminium interlayer was

introduced into the diffusion bonding process, the diffusion of elements across the bond marginally improved the interface integrity and weld strength in welds obtained at lower bonding temperatures. The sample welded at 430 ºC obtained a shear strength of 30.5 MPa for samples without interlayer and 41.5 MPa for a sample with an interlayer However, pure aluminium has poor strength, which can reduce the joint strength, especially at higher bonding temperatures. The sample welded at 520 ºC obtained a shear strength of 157.8 MPa for samples without interlayer and 148.2 MPa for the sample with an interlayer. Zhang et al. [85] reported diffusion bonding of aluminium and magnesium using a nickel interlayer. Their result shows that nickel interlayer can impede the formation of intermetallic compounds. The diffusion bonded joints were formed by Al, Ni, and Mg diffusion.

Wu et al. [9] investigated the effect of alloying elements (Mg) during diffusion bonding between aerospace aluminium alloys. It was reported that the increase in temperature increases the diffusion coefficient of magnesium. Combined with the alloying element gradient, the diffusion flux of alloying elements increases as well, which results in the improvement of the weld interface integrity and joint quality. Therefore, by increasing the alloying element diffusion flux in the interface region, weld strength enhances as well. The highest shear strength was achieved at 520 ºC (190 MPa for the 1420-7B04 couple).

(iii) Use of impulse pressure

Diffusion bonding can provide parts with a high-quality bond. However, as mentioned before, the main flaw of this solid-state technique is long processing time, usually in the order of several hours as well as the necessity of having a highly polished surface. To overcome this problem, some studies have investigated the influence of rapid variation in the applied load during the DB process [17]. This process is referred to as impulse pressure-assisted diffusion bonding (IPADB) or impulses pressuring diffusion bonding (IPDB). The first idea to use IPADB was developed and implemented at the E.O. Paton Electric Welding Institute of the National Academy of Sciences in Ukraine [86]. The implementation of this method showed improved efficiency in breaking the protective oxide layer.

5. Friction Stir (Spot) Welding

5.1. Basic principle

Friction stir welding was initially developed at The Welding Institute (TWI) of the UK in 1991 as a solid-state joining technique for joining aluminium alloys. As compared to fusion welding techniques, FSW consumes less energy and does not use involve consumables such as shielding gas or flux [87,88]. Over the years, FSW has engulfed a wide range of friction stir-assisted manufacturing processes. Some processes are intended for joining [89], while others are intended for material modification [90]. As the topic of this review paper is related to the influence of entrapped oxide layers between two or more sheets, the focus here will remain on FSW and FSSW.

The basic principle of FSW is simple. A non-consumable rotational tool is plunged into the abutting sheet edges and traversed along the joint line. After finishing the process, the tool retracts and leaves a keyhole behind. The tool consists of a specially designed probe and shoulder. Heating in the material is induced by the friction between the tool and the workpiece and due to the volumetric friction caused by the deformation of the local structure [91,92]. The friction-induced heating softens the material around the probe and below the shoulder. The proper combination of process parameters with tool geometry causes the softened material to move from the front to the back of the probe. The complex movement of the material between the tool and workpiece depends mostly on the tool geometry. FSW causes the material to undergo intense plastic deformation which increases the local temperature leading to dynamic recrystallisation in the stir zone [61]. Dynamic recrystallization produces refined microstructure in the stir zone which has a significant influence on the mechanical properties of the joints. Even though with FSW it is possible to obtain different types of joint configurations, it is mostly used for welding butt joints [93] and less frequently for lap joints [94].

Friction stir spot welding (FSSW) is a joining technique developed on the same concept as friction stir welding, but it is a spot joining technique. It is mostly used to obtain lap joints **Error! Reference source not found.** [95]. However, in some cases, it was also used for butt joining [86]. In both cases, the basic concept consists of three stages. Pin and shoulder plunging or heating stage to soften the surrounding material – heating is induced by friction at the contact interface between the workpiece

and tool during the plunging and stirring. The rotation and axial load of the tool facilitate plastic flow and stir the material. When the tool reaches a predefined plunge depth inside the material, it is held in that position for a certain time or retracted from the material leaving the FSSW joint with a keyhole [96] or without a keyhole [97], so called pin-less FSSW, depending on the tool geometry and equipment type.

5.2. Residual oxide behaviour of the friction stir (spot) welded joints

The residual oxide film in FSSW and FSW joints represent one of the biggest obstacles to obtaining defect-free joints. The influence of the entrapped oxide is reflected in the mechanical properties of the welds. One can easily observe compromised tensile, shear and fatigue strength of the joints. The effect of the residual oxide depends highly on various parameters such as equipment set-up, tool geometry, joint configuration and lesser extent from welding parameters. The most influential are joint configurations and tool geometry. Figure 5 shows most typical joint configurations that can be found in FSW and FSSW processes during butt joining with a tool using a pin. The kissing bond can be seen to distribute normally on the top surface following the spiral path of the tool.

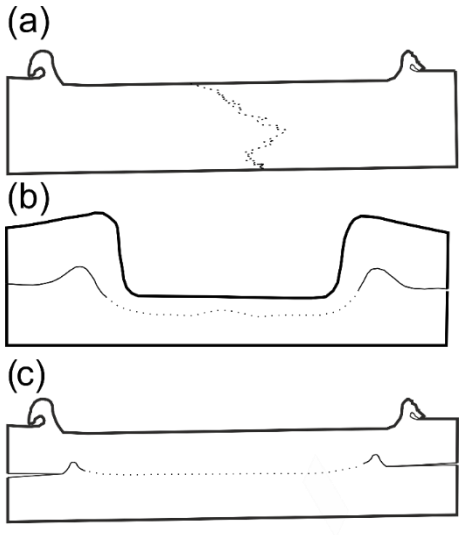

Figure 5. Schematic of the weld configurations: (a) FSW butt joint obtained with a conventional tool with a pin; (b) FSSW lap joint obtained with a conventional tool with a pin; (c) FSSW lap joint obtained with the pin-less tool.

According to Sato et al. [6,98], oxide distribution has the highest influence on the bending properties during conventional FSW. Sato et al. [6,98] were the first to systematically examine the effect of oxide on the bending properties of FSW of aluminium alloy AA 1050 and AA 5052-O by using a transmission electron microscope. According to Sato et al. [6] kissing bond was revealed in samples obtained at lower heat-input parameters in the form of a zig-zag line by using the root-bend test. The optical macrograph of the bent sample shows a zig-zag line formed in the stir zone (Figure 6(a)). The fracture during the bending test was seen to initiate from the root tip of the zig-zag line. To analyse the composition close to the zig-zag line, a TEM was used. In Figure 6(b) the TEM image of the large particle is presented. The particle was placed between the holes. Electron diffraction patterns of the particle and local material are shown in Figure 6(c,d), respectively. The particle was observed to have an amorphous structure that corresponds to the Al_2O_3 found typically on top of the aluminium sheets. According to the Energy dispersive spectroscopy (EDS) analysis, the particles consist of roughly 50% aluminium and 50% oxygen while the surrounding material consists mostly of aluminium.

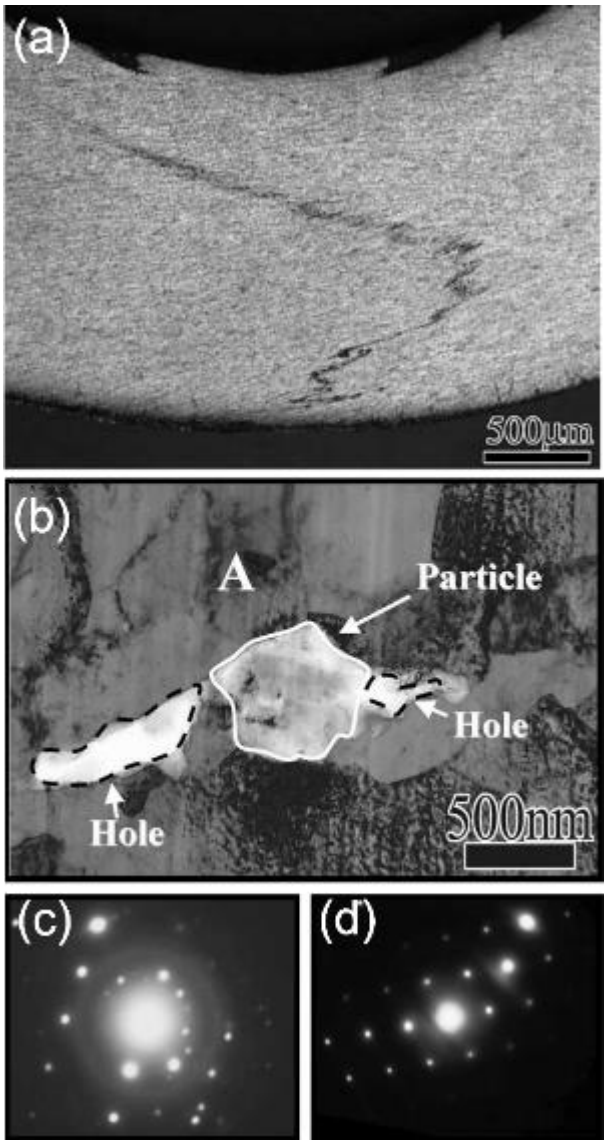

Figure 6. (a) Transmission electron microscope image of oxide particle; (b) electron diffraction pattern obtained from the particle; (c) electron diffraction pattern obtained from the matrix A [6].

In a sample welded with low heat input around the root tip of the zig-zag line, it was also found to accompany a continuous film of thickness between 10 to 100 nm (Figure 7). TEM analysis together with the EDS showed the same amorphous structure with a higher amount of oxygen compared to the surrounding aluminium. This result suggested that the continuous layer is also Al_2O_3. Cracks during the root-bending test were found in samples with lower heat input where bigger oxide particles and a continuous oxide layer were found [6].

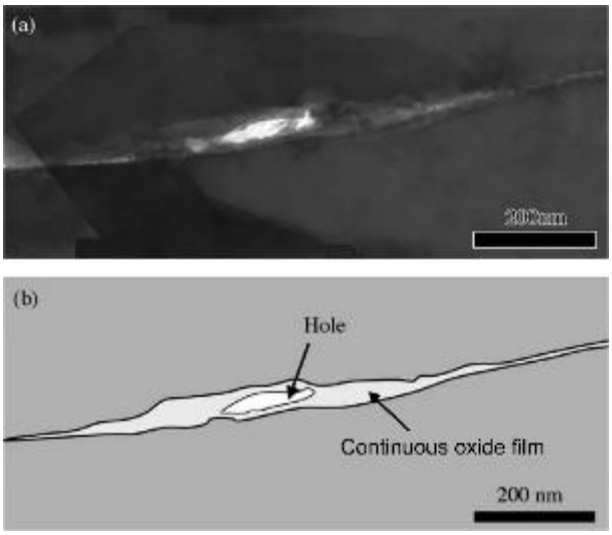

Figure 7. (a) Transmission electron microscope image of the root of the sample with low heat input; (b) schematic illustration of (a) [6].

Duong et al. [99] studied defect formation during friction stir welding of dissimilar T-lap joints between aluminium alloys AA 7075-T651 and AA 5083-H116. Even though the sheets were polished before welding with SiC paper to limit the influence of the oxide layer, it appeared in form of hook defects and kissing bond defects (Figure 8). The hook defects that appeared under the low welding rate (0.13 and 0.19 mm/rev) are shown in Figure 8(a-1) and it can be minimised by increasing the welding rate as shown in Figure 8(b-1). Hook defects emerged due to the pushing of the initial interface upward vertical material flow which gets enhanced at a low welding rate with growing heat input They affect the maximal ultimate strength and cause premature failure during the tensile test. The ultimate tensile strength of the base materials AA 7075 alloy AA 5083 alloy were 550 MPa and 320 MPa respectively and when the FSW sample failed at the hook defect line of AA 5083 side, the ultimate tensile strength was seen to be reduced to only 120 MPa.

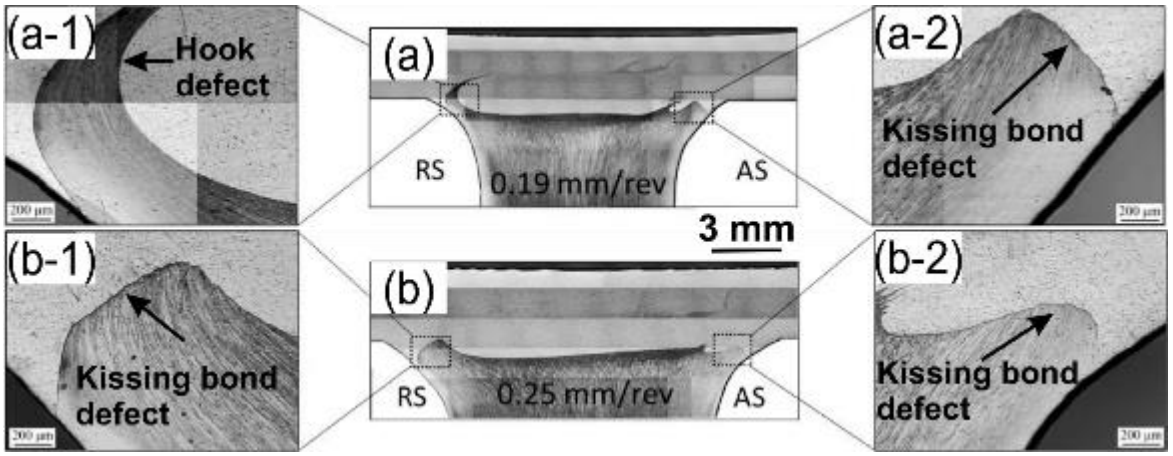

Figure 8. (a) Hook defect at 0.13 mm/rev (b) oxide film along hook defect (adapted from [99]).

Unlike butt joints, the kissing bond effect in lap joints arises at corner filets at both retreating (RS) and advancing (AS) sides as shown in Figure 8(a,b). The welding parameters does not influence the formation of kissing bonds on the size and shape. However, kissing bond defects appears in all samples and very often they are responsible for reduced fatigue strength of the welds [7,100].

Residual oxide has a higher influence on the weld properties during FSSW than FSW. FSSW is mostly used for obtaining lap joints and recently there is an emerging trend to use the pin-less tool [98–101]. When a conventional tool (with a pin) is used to weld spot lap joints, a weld zone is only a small ring area surrounding the keyhole which arose after tool retraction. This zone often contains kissing bond and hook defects due to a complex material flow resulting from the combined action of the tool pin and shoulder.

Badarinarayan et al. [102,103] studied conventional friction stir spot welding of AA 5083 and AA 5754 aluminium alloys, respectively with different tool geometries. Firstly, they explored [103] two different tools with cylindrical and triangular pins. Figure 9 show the macrostructure of welds obtained with both tools. In both welds, three characteristic regions were seen (i) completely bonded region; (ii) partially bonded region; (iii) unbonded region as shown in Figure 9(a). The completed bonded region got formed due to the severe plastic deformation caused by the rotating tool, which disperses the oxides randomly and eliminates the observation of a clear weld interface. In the partially bonded region, the oxide film becomes broken into an array of discontinuous particles. The array of oxide particles is called hook and causes the weld to be partially bonded in this region. Different

shapes of hooks were found in welds obtained with cylindrical and triangular tools. The hook in the weld obtained with cylindrical tool runs gradually upward and then bypasses the stir zone and streams downward towards the weld bottom shown in Figure 9(a1,a2). On the other hand, the welds obtained with triangular tool hook defects go directly upward towards the stir zone and ends with a very short plateau as shown in Figure 9(b1, b2). The cross-tension strength of the welds obtained with a tool with a triangular pin was 3.5 kN while welds with cylindrical tool achieved just ~2 kN.

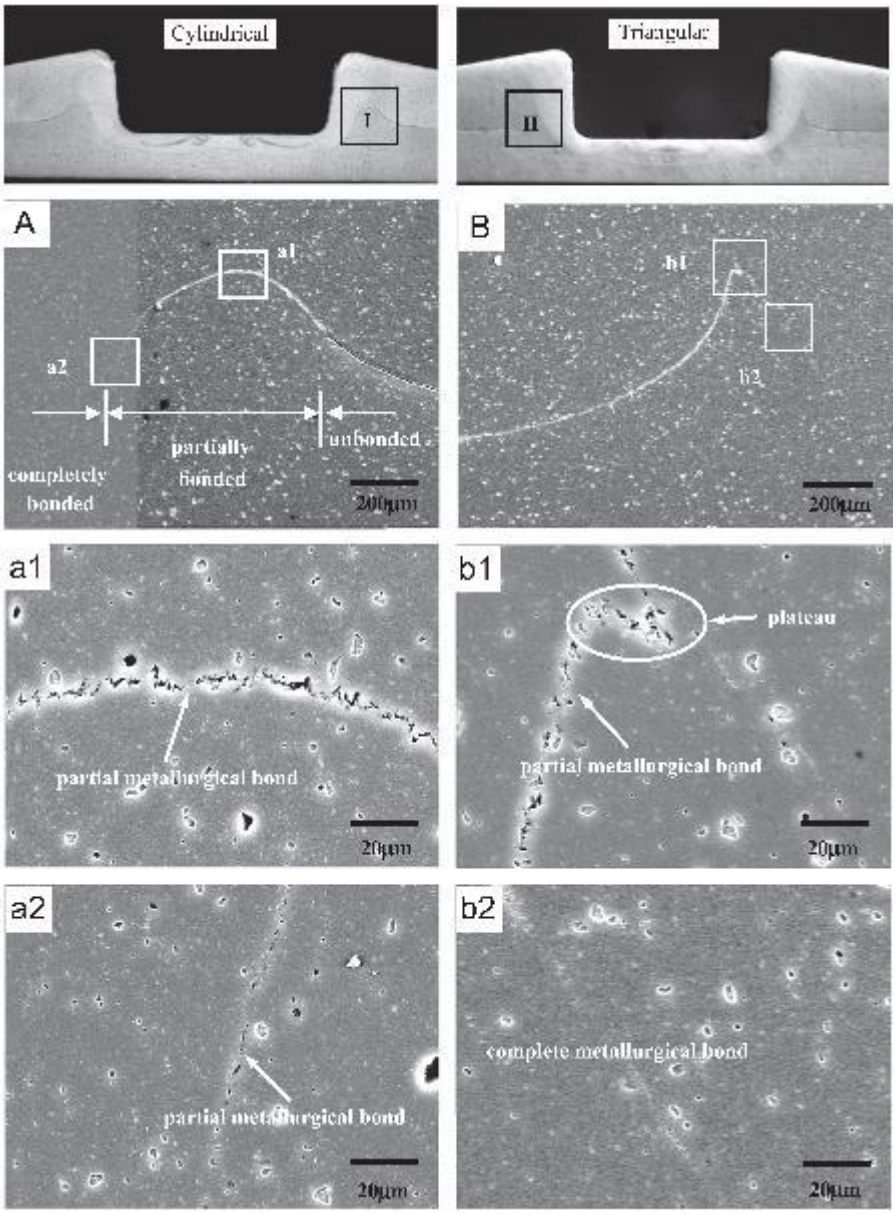

Figure 9. Cross-sectional macrostructure of the welds obtained with a cylindrical tool (left) and a triangular tool (right). (A) hook defect in a region I in weld obtained with the cylindrical tool; (B) hook defect in region II in weld obtained with the triangular tool; (a1) and (a2) partial metallurgical

bonding within the region I at indicated locations; (b1) and (b2) partial and complete metallurgical bonding in region II at indicated locations [102].

Shen et al. [22] studied conventional FSSW of aluminium alloy AA 6061-T4 lap joint between two sheets with 2 mm thickness. They found hook and kissing bond defects at the periphery of the stir zone. Hook defect was observed to originate from the region between the overlapped metal sheets, spreads upward towards the weld, and finally disappear in the periphery of the stir zone. This was caused by the flow of material into the upper sheet from the lower sheet, which was caused by the penetration of the tool into the bottom sheet. A kissing bond defect was also observed as a transition zone between the completely bonded region and the no-contact region. In those regions, residual oxide breaks into particles due to the continuous tool stirring motion and becomes dispersed into the weld region causing a partial metallurgical bond. Higher stir time caused more uniform oxide distribution and mechanical properties for all rotational speeds. The highest difference can be observed in samples welded at 1500 RPM. Samples joined for a welding duration of 2 s showed strength of 1800 MPa, while samples joined with a welding time of 4 s showed a strength of 4500 MPa. Zhang et al. [104] and Yang et al. [105] had similar observations during the FSSW of aluminium alloy AA 5052 and magnesium alloy AZ31, respectively. The only difference was in the shape and size of hook defects which can be correlated to tool geometry. Those defects combined with a keyhole in the middle of the joint significantly reduce the mechanical properties of the joints which were one of the main reasons to seek different solutions such as FSSW with pin-less tool [106–108] or novel methods such as refill FSSW [109–112].

The pin-less tool proved to be a superior alternative compared to a conventional tool with a pin because it does not leave a keyhole in the joint at the end of the process. A keyhole reduces mechanical properties [101,108] and becomes a potential site for corrosion [113–115]. However, a pin-less tool usually penetrates only into the first sheet, which causes less or no stirring at the bond interface. The joining mechanism mostly relies on diffusion between the sheets. In this case, the only mechanism for disturbing the oxide layer is stretching the bond line due to the tool rotation, pressure and interaction between asperity tips between the sheet surfaces. Therefore, the oxide layer stays

entrapped between the weld interface which impedes diffusion between the sheets, causing poor welding properties and in some cases delamination [4,46,116].

Welding parameters, tool geometry and equipment set-up have a significant influence on the distribution of oxides and therefore mechanical properties during FSSW. The right combination of those variables can cause higher stretching of the welding line which can cause higher disruption of oxide and therefore wider surface where diffusion can occur. Figure 10 shows the influence of tool geometry and equipment set-up on shear load during different types of FSSW reported in different studies. A few special FSSW processes are presented as well, such as pinless- (PLT-FSSW) [5], walking- (WFSSW) [104]; protrusion- (PFSSW) [117]; flat- (FFSSW) [31] and refill- (RFSSW) [118] friction stir spot welding. The studies presented in Figure 10were made on 5xxx aluminium alloy. It can be seen that refill friction stir spot welding (RFSSW) produces welds with the highest strengths. The process was developed as an improvement to the conventional FSSW to avoid keyholes andhook defects. Welds performed on the same base material (5083-O) and with slight difference in thickness (1.6 and 2 mm), resulted in a shear force that differed significantly. With RFSSW, joints were seen to achieve more than 7 kN tensile shear force, while conventional FSSW samples attained just ~4 kN. Andalib et al. [31] showed that a special flat FSSW set-up under the same conditions yields a higher tensile shear force (~6 kN) compared to CFSSW (~4 KN). Low strength in the CFSSW process was ascribed sto the kissing bond effect resulting from a continuous layer of oxide.

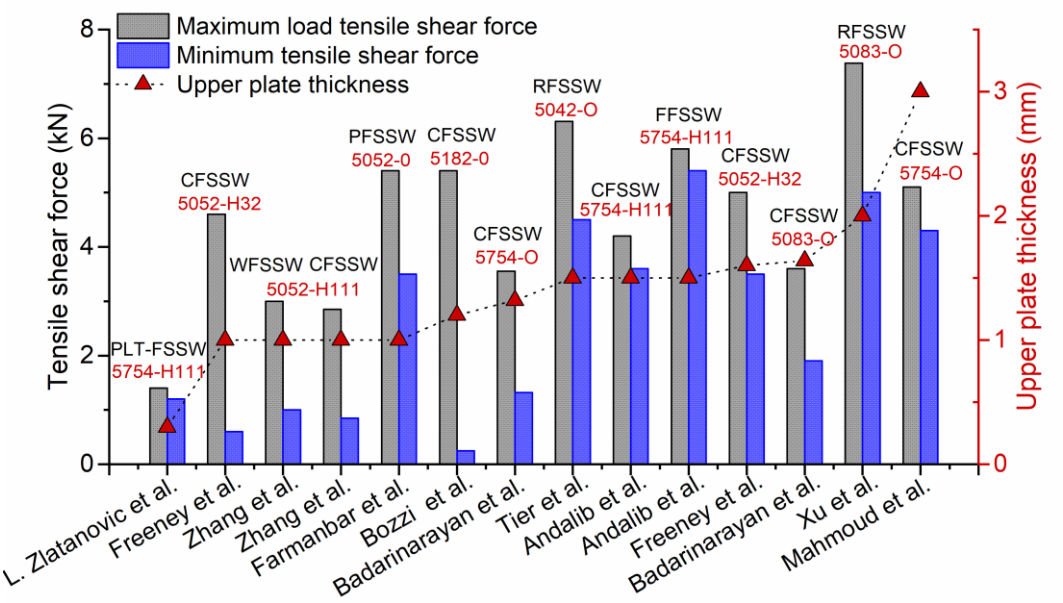

Figure 10 Comparative plots of maximum and minimum tensile shear forces of welding samples by different types of FSSW and different aluminium alloys from 5xxx series (PLT-FSSW – pinless tool friction stir spot welding; CFSSW – conventional FSSW; WFSSW - walking FSSW; PFSSW – protrusion FSSW; FFSSW – flat FSSW; RFSSW – Refill FSSW) [5,31,103,110,117–121].

Labus Zlatanovic et al. [4,5] studied the morphology and properties of the weld faying interface of aluminium alloy fabricated using after FSSW (AA 5754-H111). Four sheets of 0.3 mm thickness were welded with the convex pin-less tool. Figure 11(a,b) shows a specimen welded at low rotational speed (low heat input) with a complex layer consisting of oxides of Al_2O_3, MgO and intermetallics (Al_3Mg_2 and $Al_6(FeMn)$) at the weld faying interface. Also, in the same region, a higher volume of dislocations and a more refined grain structure compared to the stir zone were observed. It is worth noting that in the middle of the joints, several nano and micro pits were observed. Those pits were surrounded by residual oxide, which initially impeded diffusion and left pits in places with high concentrations of oxide particles. However, in the sample welded with low heat input shown in Figure 11(c,d), the lowest spots were dynamically precipitated intermetallics on the periphery between recrystallised zone (RZ) and weld faying interface (WFI). However, in samples welded at high temperatures, dynamic recovery took place and in WFI only residual oxide particles and nano and micro pits were seen. Higher volume and the size of the pits were observed in this specimen and a thicker residual oxide

layer which significantly influences the mechanical and electrical properties of the weld. The sample welded at 4500 RPM (higher heat input) showed a lower strength of ~1.2 kN and higher electrical resistance compared to the sample welded at 1000 RPM (lower heat input) where shear strength was 1.4 kN. This implies that the oxide layer combined with nano and micro pits increases electrical resistivity as both Al_2O_3 and MgO have high electrical resistance [122].

In summary, it can be deduced that the residual oxide layer in FSW and FSSW welds can trigger the formation of various types of defects such as kissing bond, hook and nano and micro pits at the weld faying interface. Those defects influence the mechanical properties (fatigue, shear and tensile strength, bending properties) and electrical properties of FSW and FSSW welds. Most research in the field of FSW and FSSW used optimisation of process parameters and tool geometry to suppress its adverse impact. However, no engineering solution has completely solved this problem.

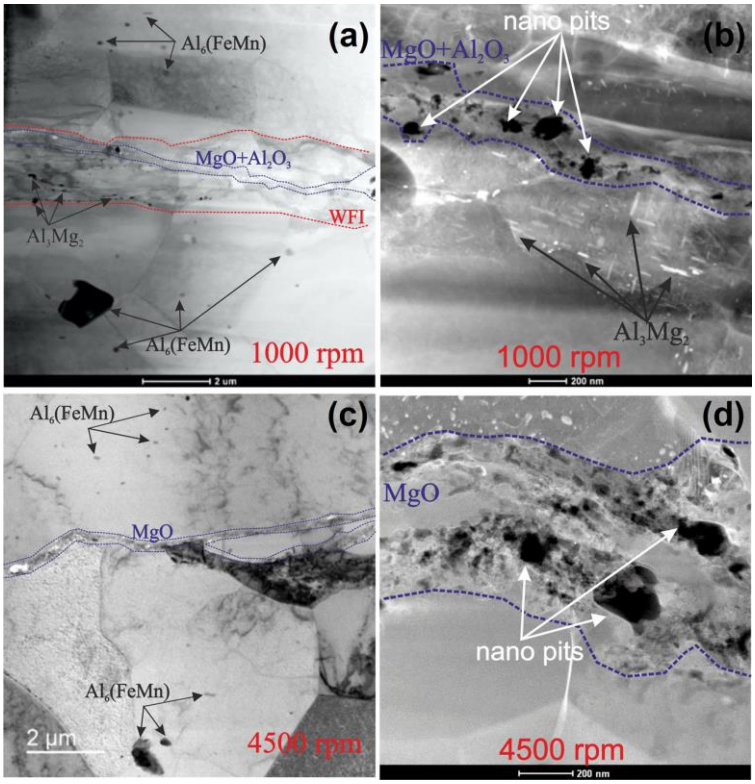

Figure 11. Scanning transmission electron macrographs of weld faying interface: (a) bright field of sample welded with low heat input – 1000 rpm (lower magnification); (b) annular dark-field image of (a) (higher magnification); (c) bright field of sample welded with high heat input – 4500 rpm (lower magnification); d high-angle annular dark-field image of (c) (higher magnification) [5].

6. Ultrasonic welding

6.1. Basic principle

USW was first introduced in 1950 for welding thin foils, wire bonding and tube sealing [123]. Over the years, advancements in welding systems have led to significant development in the ultrasonic equipment in a way to provide the possibility to join thicker metal sheets (up to 3 mm). Above 3 mm sheet thickness, the heat generation and relative motion at the weld interface are poor. Therefore, it is usually used to bond small parts in electronics, medical tools, watches etc. However, the main application of USW is in the automotive industry [124–126].

Ultrasonic welding (USW) is a solid-state welding technique that utilises high-frequency mechanical vibrations to generate friction-like relative motion between the two workpieces [127]. It results in local plastic deformation and shearing of surface asperities that transfer contaminations and oxides to promote local heat generation, increasing the temperature at the weld interface. High local temperature decreases the local yield strength at the weld interface and causes local microplastic deformation. Thereafter, localised adhesion and micro-joints are created, and eventually expand over the entire weld faying interface [123,128].

USW is used for welding lap joints, and various weld configurations can be achieved (spot, torsion or roll seam welds) by different machine and tool (sonotrode) designs. The basic principle is the same. Sheets are pressed between the tool and anvil during the process to obtain weld joints. The employed process parameters mainly affect the microstructure and mechanical properties of the USWed joints [127,129].

Ultrasonic vibrations generate friction between workpieces resulting in a closer contact between two interfaces with simultaneous local friction heating of the contact area. The interatomic bond formed by USW, under these conditions provides high-strength joints with short welding time (<1s for spot welding of metals) and low energy input.

In the extant literature, it is considered that the aluminium oxide layer between the sheets, which are ultrasonically welded, becomes fragmented in a way that the diffusion between the fragments remains

undisturbed. However, the influence of those distributed aluminium fragments on weld quality and electrical properties is studied only up to a limited extent.

6.2. Residual oxide behaviour inside ultrasonically welded joints

Weld strength of ultrasonically welded metal specimens is derived from two phenomena, namely the surface- (friction) and volume- (plasticity) softening effect [130,131]. The surface softening effect is caused by the interfacial friction between two mating surfaces, while the volume softening effect involves the inner stresses and plastic deformation during welding. Most USW operations are governed by surface effect, whereby under oscillatory vibrations the friction and bonding mechanisms depend on applied load, surface topography, the oxide film nature, and the relative oxide- and metal substrate- hardness. Fewer studies were performed to understand the volumetric softening effect because it directly influences conventional welding operations [131,132].

To break up the oxide film on the welding interface during the USW process, welding pressure is applied to the sonotrode, which alters the shear stress. Those stresses produce elastic-plastic deformation of surface asperities. Due to plastic deformation, the oxide film breaks, and metal-to-metal bonding is achieved, followed by atomic diffusion. The broken fragments of oxide film disperse nicely in the vicinity of the weld interface or inside the weld zone [133,134]. Therefore, the dispersed oxide particles have a significant influence on the microstructural and mechanical properties of the weld, usually preventing atomic diffusion to occur in some parts of the weld interface (Figure 12).

Li et al. [133] found that process parameters such as welding pressure play a significant role. A joint welded by using 1575 N clamping pressure obtained a maximum strength and the strength degrade beyond this pressure.

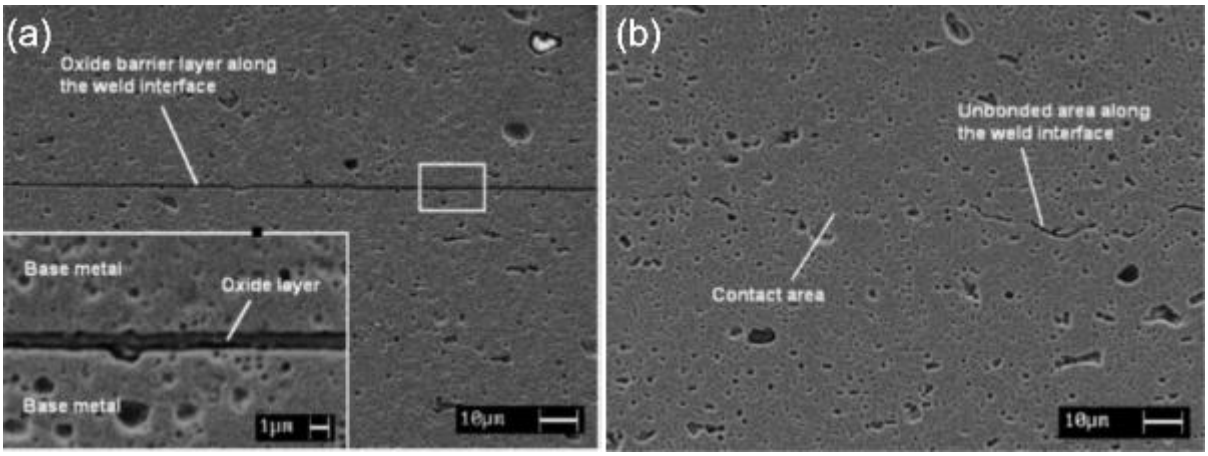

Figure 12. Scanning electron images of aluminium alloy (AA 6061) specimen obtained with ultrasonic consolidation process (a) an unclean specimen showing ~500 nm thick oxide film along with weld interface. Insert shows magnification of the residual oxide layer (b) weld interface with contact area and oxides dispersed along with the interface [134].

Kong et al. [134,135] studied ultrasonic consolidation (UC) of aluminium alloys. In theirstudy[134], uncleaned (unprepared) aluminium alloy AA 6061 specimens welded with a thick oxide layer and the cleaned specimens, with a removed oxide layer were explored. Specimens were cleaned with degreaser – petroleum distillate and wiped with a clean cotton cloth to remove oxides and impurities. The uncleaned specimen shown in Figure 12a showed no clear metallurgical bond between the sheets. The residual oxide film at the weld interface causing poor bonding was observed. In these specimens peeling test caused separation along the whole length. Specimens prepared with surface cleaning also showed some oxide remains at the weld interface. Figure 12b shows the clean bond (contact points) and unbonded area dispersed along with the weld interface. The cleaning of the surfaces before bonding caused increased linear weld density by up to 45%. However, the peel test strength was similar with and without sample preparation. Parameters had a high influence on mechanical properties. However, a significantly higher deviation in the peeling load of unprepared samples can be observed compared to prepared samples. For example, in samples welded with 43.5 mm/s and 241 kPa, the difference between the minimum and maximum peel load in batches obtained with different amplitudes was 16 N while in batches welded with the same parameters on prepared samples was 8 N. However, during ultrasonic welding of aluminium alloy AA 3003 [135], highly localised, oscillating

shear forces were reported to break up oxide film and contaminations on the foil surfaces, permitting diffusion between two clean metal surfaces to occur. No additional cleaning of the samples was done. Load was applied to the weld area as a combined static and oscillating shear load which causes dynamic internal stresses at weld interfaces. Furthermore, it causes elastic-plastic deformation and allows atomic diffusion across the interface. The broken surface layer was displaced in the vicinity of the interface, or it is interrupted in random areas within the weld zone. The maximal peeling load achieved was 105 N, while in [134] the maximal obtained peeling load was 72 N.

Mariani et al. [39] also studied ultrasonic consolidation of aluminium alloy (AA 6061-O) with SiC fibre embedded between the sheets. Like the previous research, ultrasonic oscillations break and disperse residual oxide film and the core of the welding zone is characterized by a strong metallic bonding.

Watanabe et al. [136] studied the influence of surface oxide film during the ultrasonic welding of dissimilar metal alloys namely aluminium (A1050P) with copper (C1220P) and aluminium with austenitic stainless steel (SUS304). Furthermore, the influence of oxide film on weld strength and the welding process was investigated. For the aluminium-copper joints, weld strength decreases with the increase of the copper oxide film thickness. The electrolytically polished samples had an ultimate tensile strength of ~200 N while the samples after oxidation at 300 ^{o}C attained just ~50 N. However, the thick aluminium oxide layer causes a decrease in the ultimate tensile strength of only ~20 N (from ~200N for electrolytically polished samples to ~180 N for samples with AlO_5 oxide layer 1250 nm thick) . Also, for aluminium-steel joints, no decrease in weld strength was observed with an increase in aluminium oxide thickness. In aluminium-copper specimens, aluminium oxide rupture locally and the welding area increases with the laps of the processing time. In aluminium-steel specimens, aluminium oxide ruptures over the wide range at the onset of joining, and welding area and weld strength increase.

Fujii et al. [137] studied the behaviour of the aluminium oxide layer at the weld interface during the USW of aluminium and copper. To observe the oxide behaviour, the non-anodized and anodized aluminium alloy AA 1050 was used. Material flow during USW together with mechanical mixing

broke and dispersed the oxide film into the aluminium substrate (Figure 13). Welding time had a high influence on dispersing the aluminium oxide and on the peel strength. Therefore, samples that were welded with welding time up to 0.35s suffered interfacial debonding, while samples welded with higher welding time fractured in the base material. Anodized samples had a lower tensile shear strength compared to the non-anodized samples for all different welding times. The highest tensile shear strength of ~1.1 kN was obtained with a non-anodized sample for a welding time of 0.4 s, while for the same conditions anodized sample obtained ~1 kN.

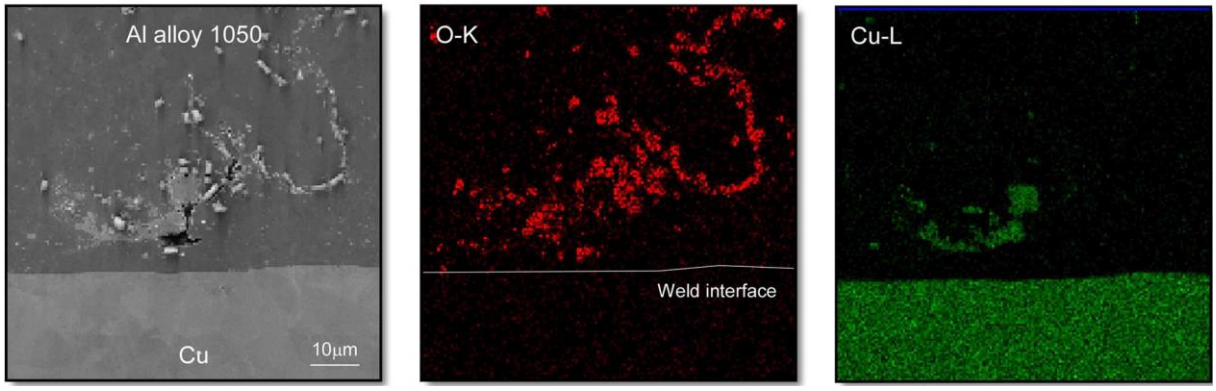

Figure 13. Scanning electron microscope images at the weld interface of ultrasonic welded Al/Cu specimen with elemental maps of the area presented in SEM image obtained with Energy-dispersive X-ray spectroscopy (adapted from [137]).Matsuoka et al. [138] had a similar observation during the study of ultrasonic welding of aluminium-copper joints. With welding parameters, it is possible to disperse the residual oxide layer within the weld zone which allows metal-to-metal contact and atomic diffusion to occur.

In many ultrasonic welding studies, the oxide layer was mentioned as a reason for partial bonding, or as a defect that reduces joining strength. It was mostly mentioned as an assumption or referring to previous research. However, no direct correlation with the presented results was drawn [132,139–141].

7. Concluding remarks

Solid-state welding techniques are very popular for welding aluminium alloys in the transportation industry. The major drawback of these techniques is the chemically stable residual oxide layer

entrapped in the welding interface causing compromised weld properties. This paper reviews the fundamental understanding of the oxide behaviour within solid-state welded joints made of aluminium alloys. Solid-state techniques analysed in this paper were diffusion bonding, friction stir spot welding and ultrasonic welding and the following conclusion were drawn:

Aluminium alloys used in the transportation industry have a chemically stable protective layer which causes poor bonding, especially in solid-state bonding processes as the melting points of oxide differ significantly from pristine materials. Those residual oxides inside welds trigger defect formations (pits, voids, delamination, etc.). Aluminium oxide grows very fast (in less than a second) so even after removing from the surface prior to welding, a thin layer gets developed almost immediately.

To weld- in solid-state two aluminium workpieces together a metal-to-metal contact is required. Therefore, all impurities and oxides must be highly interrupted for diffusion to occur. From all proposed models, the model proposed by film theory show the highest level of agreement to all solid-state processes. However, the assumption is that in most solid-state processes more than one model is involved.

The highest influence of residual oxides is observed during diffusion bonding because the lowest level of deformation is applied to the weld interface, which is an important factor in the oxide interruption process. All the proposed approaches interrupt the oxide layer and improve bonding and mechanical properties. However, there is always a partial bonding, because one portion of the oxide layer is always present. Bonding temperature and pressure were the most influential parameters on weld strength. However

Friction stir (spot) welding induces a high level of deformation on the weld interface. Especially when FSW with a conventional tool with a pin is used. As the weld interface is severely deformed, the residual oxide gets dispersed in the weld zone. However, as being still present in the joint it influences weld properties. To reduce its influence during FS(S)W optimisation of the process parameters and tool geometry was used. The most influential process parameters on oxide interruption are rotational speed, welding speed, process time andapplied load. Tool geometry and equipment setup also play an important role. Weld strength is highly influenced by a combination of all those variables together. In

ultrasonically welded aluminium specimens, to break the oxide film at the welding interface, welding pressure is applied which interacts with the shear stress. Those stresses produce elasto-plastic deformation of the surface asperities. Due to the plastic deformation, the oxide film breaks, and metal-to-metal bonding is achieved, followed by atomic diffusion. Oxide film broken during the process is dispersed in the vicinity of the weld interface or inside the weld. The most influential parameters affecting the oxide interruption and weld strength are process time and welding pressure.

Even though many researchers have studied this topic, the problem of residual oxide in solid-state welded joints remains unsolved completely, which needs attention. This is an acute problem with relevance to technology and a challenge that spurs across multidisciplinary themes and needs engineers from the field of joining and chemistry to work together to eliminate the issue of oxide formation to achieve a seamlessly sustainable manufacturing using solid-state technique.

The work in future can consider innovating hybrid methods involving use of vibration frequencies during diffusion bonding and friction stir welding. The development of newer types of fluxing agents capable of decomposing the oxide layer during the welding processes at elevated temperatures can be one of the possible solutions to suppress the negative influence of residual oxides.

Acknowledgements

The authors gratefully acknowledge research support by the project entitled “Materials, joining and allied technologies” in the Department of Production Engineering, Faculty of Technical Sciences Novi Sad, Serbia.

Disclosure statement

No potential conflict of interest was reported by the author(s).

References

[1] Oliveira PHF, Amancio-Filho ST, Dos Santos JF, et al. Preliminary study on the feasibility of friction spot welding in PMMA. Mater Lett [Internet]. 2010;64:2098–2101. Available from: http://dx.doi.org/10.1016/j.matlet.2010.06.050.

[2] Akinlabi ET, Mahamood RM, Akinlabi SA, et al. Processing Parameters Influence on Wear

Resistance Behaviour of Friction Stir Processed Al-TiC Composites. 2014;2014.

[3] Chu Q, Yang XW, Li W, et al. Microstructure and mechanical behaviour of pinless friction stir spot welded AA2198 joints. Sci Technol Weld Join. 2016;21:164–170.

[4] Labus Zlatanovic D, Balos S, Bergmann JP, et al. In-depth microscopic characterisation of the weld faying interface revealing stress-induced metallurgical transformations during friction stir spot welding. Int J Mach Tools Manuf. 2021;103716.

[5] Labus Zlatanovic D, Bergmann JP, Balos S, et al. Influence of rotational speed on the electrical and mechanical properties of the friction stir spot welded aluminium alloy sheets. Weld World [Internet]. 2022; Available from: https://link.springer.com/10.1007/s40194-022-01267-8.

[6] Sato YS, Takauchi H, Park SHC, et al. Characteristics of the kissing-bond in friction stir welded Al alloy 1050. Mater Sci Eng A. 2005;405:333–338.

[7] Kadlec M, Ruzek R, Chatzakos P, et al. Influence of the Kissing Bond Defect to the Fatigue Life in Friction Stir Welds of AA7475-T7351 Aluminium Alloy [Internet]. 2014. Available from: https://www.researchgate.net/publication/271763178.

[8] Shirzadi AA, Assadi H, Wallach ER. Interface evolution and bond strength when diffusion bonding materials with stable oxide films. Surf Interface Anal. 2001;31:609–618.

[9] Wu F, Zhou W, Han Y, et al. Effect of alloying elements gradient on solid-state diffusion bonding between aerospace aluminum alloys. Materials (Basel). 2018;11.

[10] Phillips DH. Solid-State Welding Processes. Weld Eng An Introd. Springer; 2015. p. 95–113.

[11] Hill A, Wallach ER. Modeling solid-state diffusion bonding. Acta Metall. 1989;37:2425–2437.

[12] Dunford D V., Partridge PG. Strength and fracture behaviour of diffusion-bonded joints in Al-Li (8090) alloy - Part II Fracture behaviour. J Mater Sci. 1991;26:2625–2629.

[13] Noonan JR, Davis HL. Atomic Arrangements at Metal Surfaces. Science (80-). 2016;234:310–316.

[14] Cooper DR, Allwood JM. The influence of deformation conditions in solid-state aluminium welding processes on the resulting weld strength. J Mater Process Technol [Internet]. 2014;214:2576–2592. Available from: http://dx.doi.org/10.1016/j.jmatprotec.2014.04.018.

[15] Cabibbo M, Paoletti C, Ghat M, et al. Post-FSW cold-rolling simulation of ECAP shear deformation and its microstructure role combined to annealing in a FSWed AA5754 plate joint. Materials (Basel). 2019;12:1–14.

[16] Bagheri B, Mahdian Rizi AA, Abbasi M, et al. Friction Stir Spot Vibration Welding: Improving the Microstructure and Mechanical Properties of Al5083 Joint. Metallogr Microstruct Anal [Internet]. 2019;8:713–725. Available from: https://doi.org/10.1007/s13632-019-00563-y.

[17] Alhazaa A, Haneklaus N, Almutairi Z. Impulse pressure-assisted diffusion bonding (IPADB): Review and outlook. Metals (Basel). 2021;11:1–9.

[18] Macwan A, Mirza FA, Bhole SD, et al. Similar and Dissimilar Ultrasonic Spot Welding of 5754 Aluminum Alloy for Automotive Applications. Mater Sci Forum. 2017;877:561–568.

[19] Hamilton CH. Bonding of berylium members. United States Pat. Off. 1969.

[20] Yamamoto M, Matsumae T, Kurashima Y, et al. Comparison of argon and oxygen plasma treatments for ambient room-temperature wafer-scale au-au bonding using ultrathin au films. Micromachines. 2019;10.

[21] Mhich A. Laser cleaning prior to diffusion bonding of the Ti-6Al-4V for aerospace applications A thesis submitted to The University of Manchester for the degree of Doctor of Philosophy in

the Faculty of Engineering and Physical Science School of Materials. University of Manchester; 2015.

[22] Shen Z, Yang X, Zhang Z, et al. Mechanical properties and failure mechanisms of friction stir spot welds of AA 6061-T4 sheets. Mater Des [Internet]. 2013;49:181–191. Available from: http://dx.doi.org/10.1016/j.matdes.2013.01.066.

[23] Koyama S, Takahashi M, Ikeuchi K. Behavior of Superficial Oxide Film at Solid-State Diffusion-Bonded Interface of Tin. Mater Trans. 2004;45:300–302.

[24] Pilling J. The kinetics of isostatic diffusion bonding in superplastic materials. Mater Sci Eng. 1988;100:137–144.

[25] Wang X, Gao Y, McDonnell M, et al. On the solid-state-bonding mechanism in friction stir welding. Extrem Mech Lett [Internet]. 2020;37:100727. Available from: https://doi.org/10.1016/j.eml.2020.100727.

[26] Cooper DR, Allwood JM. Influence of diffusion mechanisms in aluminium solid-state welding processes. Procedia Eng [Internet]. 2014;81:2147–2152. Available from: http://dx.doi.org/10.1016/j.proeng.2014.10.300.

[27] Rahaman MN. Kinetics and mechanisms of densification. Sinter Adv Mater. Woodhead publishing; 2010. p. 33–64.

[28] Semenov AP. The phenomenon of seizure and its investigation. Wear. 1961;4:1–9.

[29] Merstallinger A, Holzbauer R, Bamsey N. Cold welding in hold down points of space mechanisms due to fretting when omitting grease. Lubricants. 2021;9.

[30] Huang K, Logé RE. A review of dynamic recrystallization phenomena in metallic materials. Mater Des [Internet]. 2016;111:548–574. Available from: http://dx.doi.org/10.1016/j.matdes.2016.09.012.

[31] Andalib H, Farahani M, Enami M. Study on the new friction stir spot weld joint reinforcement technique on 5754 aluminum alloy. Proc Inst Mech Eng Part C J Mech Eng Sci. 2018;232:2976–2986.

[32] Jata K, Semiatin S. Continuous dynamic recrystallization during friction stir welding of high strength aluminum alloys. Scr Mater. 2000;43:743–749.

[33] Labus Zlatanovic D, Baloš S, Bergmann JP, et al. Influence of Tool Geometry and Process Parameters on the Properties of Friction Stir Spot Welded Multiple (AA 5754 H111) Aluminium Sheets Danka. Materials (Basel). 2021;14.

[34] Sharma C, Dwivedi DK, Kumar P. Effect of welding parameters on microstructure and mechanical properties of friction stir welded joints of AA7039 aluminum alloy. Mater Des [Internet]. 2012;36:379–390. Available from: http://dx.doi.org/10.1016/j.matdes.2011.03.058.

[35] Bagheri B, Abbasi M, Abdollahzadeh A, et al. Advanced Approach to Modify Friction Stir Spot Welding Process. Met Mater Int [Internet]. 2019; Available from: https://doi.org/10.1007/s12540-019-00416-x.

[36] Gerlich A, Su P, Yamamoto M, et al. Effect of welding parameters on the strain rate and microstructure of friction stir spot welded 2024 aluminum alloy. J Mater Sci. 2007;42:5589–5601.

[37] Cao JY, Wang M, Kong L, et al. Microstructure, texture and mechanical properties during refill friction stir spot welding of 6061-T6 alloy. Mater Charact J [Internet]. 2014;128:54–62. Available from: http://dx.doi.org/10.1016/j.matchar.2017.03.023.

[38] Sriraman MR, Babu SS, Short M. Bonding characteristics during very high power ultrasonic additive manufacturing of copper. Scr Mater [Internet]. 2010;62:560–563. Available from:

http://dx.doi.org/10.1016/j.scriptamat.2009.12.040.

[39] Mariani E, Ghassemieh E. Microstructure evolution of 6061 O Al alloy during ultrasonic consolidation : An insight from electron backscatter diffraction. Acta Mater [Internet]. 2010;58:2492–2503. Available from: http://dx.doi.org/10.1016/j.actamat.2009.12.035.

[40] Gunduz IE, Ando T, Shattuck E, et al. Enhanced diffusion and phase transformations during ultrasonic welding of zinc and aluminum. Scr Mater. 2005;52:939–943.

[41] Panteli A, Robson JD, Brough I, et al. The effect of high strain rate deformation on intermetallic reaction during ultrasonic welding aluminium to magnesium. Mater Sci Eng A [Internet]. 2012;556:31–42. Available from: http://dx.doi.org/10.1016/j.msea.2012.06.055.

[42] Ward AA, Zhang Y, Cordero ZC. Junction growth in ultrasonic spot welding and ultrasonic additive manufacturing. Acta Mater [Internet]. 2018;158:393–406. Available from: https://doi.org/10.1016/j.actamat.2018.07.058.

[43] Kelly GS, Advani SG, Gillespie JW, et al. A model to characterize acoustic softening during ultrasonic consolidation. J Mater Process Technol [Internet]. 2013;213:1835–1845. Available from: http://dx.doi.org/10.1016/j.jmatprotec.2013.05.008.

[44] Hu J, Shimizu T, Yoshino T, et al. Evolution of acoustic softening effect on ultrasonic-assisted micro/meso- compression behavior and microstructure. Ultrasonics [Internet]. 2020;107:106107. Available from: https://doi.org/10.1016/j.ultras.2020.106107.

[45] Mayer M, Schwize J. Thermosonic Ball Bonding Model based on Ultrasonic Friction Power. 5th Electron Packag Technol Conf (EPTC 2003). Singapore; 2003. p. 738–743.

[46] Labus Zlatanovic D, Balos S, Bergmann JP, et al. An experimental study on lap joining of multiple sheets of aluminium alloy (AA 5754) using friction stir spot welding. Int J Adv Manuf Technol [Internet]. 2020;107:3093–30107. Available from: http://dx.doi.org/10.1007/s00170-020-05214-z.

[47] Vargel C. Corrosion of Aluminium. Corros. Alum. Elsevier; 2004.

[48] Labus Zlatanovic D. Friction stir spot welding of ultrathin sheets made of aluminium – magnesium alloy, PhD thesis. University of Novi Sad; 2020.

[49] Polmaer I. Light Alloys. Fourth edi. Elsevier. Elsevier; 2006.

[50] Bagheri B, Abbasi M, Abdollahzadeh A, et al. Advanced Approach to Modify Friction Stir Spot Welding Process. Met Mater Int. 2019;

[51] Rodrigues DM, Loureiro A, Leitao C, et al. Influence of friction stir welding parameters on the microstructural and mechanical properties of AA 6016-T4 thin welds. Mater Des [Internet]. 2009;30:1913–1921. Available from: http://dx.doi.org/10.1016/j.matdes.2008.09.016.

[52] Sato YS, Urata M, Kokawa H. Parameters Controlling Microstructure and Hardness during Friction-Stir Welding of Precipitation-Hardenable Aluminum Alloy 6063. Metall Mater Trans A. 2002;33A:625–635.

[53] Flötotto D, Wang ZM, Jeurgens LPH, et al. Intrinsic stress evolution during amorphous oxide film growth on Al surfaces. Appl Phys Lett. 2014;104.

[54] Jeurgens LPH, Sloof WG, Tichelaar FD, et al. Growth kinetics and mechanisms of aluminum-oxide films formed by thermal oxidation of aluminum. J Appl Phys. 2002;92:1649–1656.

[55] Jeurgens LPH, Sloof WG, Tichelaar FD, et al. Thermodynamic stability of amorphous oxide films on metals: Application to aluminum oxide films on aluminum substrates. Phys Rev B. 2000;62:4707–4719.

[56] Reichel F, Jeurgens LPH, Mittemeijer EJ. The thermodynamic stability of amorphous oxide

overgrowths on metals. Acta Mater. 2008;56:659–674.

[57] Snijders PC, Jeurgens LPH, Sloof WG. Structure of thin aluminium-oxide ®lms determined from valence band spectra measured using XPS. Surf Sci [Internet]. 2002;496:97–109. Available from: www.elsevier.com/locate/susc.

[58] Nguyen L, Hashimoto T, Zakharov DN, et al. Atomic-Scale Insights into the Oxidation of Aluminum. ACS Appl Mater Interfaces. 2018;10:2230–2235.

[59] Beilby G. Aggregation and flow of solids. London: Macmillan and Co.; 1921.

[60] Finch GI, Quarrell AG. The Beilby Layer. Nature. 1936;516–519.

[61] Samuels L. Metallographic Polishing by Mechanical Methods. ASM: Cleveland, Ohio, OH; 1982.

[62] Leth-Olsen H. Filiform corrosion of painted aluminium coil materials, PhD thesis. Norwegian University of Science and Technology; 1996.

[63] Fishkis M, Lin JC. Formation and evolution of a subsurface layer in a metalworking process. Wear. 1997;206:156–170.

[64] Scamans GM, Frolish MF, Rainforth WM, et al. The ubiquitous beilby layer on aluminium surfaces. Surf Interface Anal. 2010. p. 175–179.

[65] Lee KS, Kwon YN. Solid-state bonding between Al and Cu by vacuum hot pressing. Trans Nonferrous Met Soc China (English Ed. 2013;23:341–346.

[66] Akca E, Gursel A. Influences of argon gas shielding on diffusion bonding of Ti-6Al-4V alloy to aluminum. Rev Metal. 2017;53.

[67] Özdemir N, Bilgin B. Interfacial properties of diffusion bonded Ti-6Al-4V to AISI 304 stainless steel by inserting a Cu interlayer. Int J Adv Manuf Technol. 2009;41:519–526.

[68] Conrad H, Rice L. The cohesion of previously fractured Fcc metals in ultrahigh vacuum. Metall Trans. 1970;1:3019–3029.

[69] Hosford WF, Caddell RM. Metal Forming - Mechanic and Metallurgy. 4th Editio. Cambridge University Press; 2011.

[70] Shirzadi A. Diffusion Bonding Aluminium Alloys and Composites : New Approaches and Modeling. Univeristy of Cambridge. Univeristy of Cambridge; 1997.

[71] Urena A, Gomez de Salazar JM, Escalera MD. Diffusion bonding of discontinuously reinforced SiC/Al matrix composites: the role of interlayers. Key Eng Mater. 1995;104–107:523–540.

[72] Tensi HM, Wittmann M. Effects of Surface Finish on the Solid State Welding of High Strength Aircraft and Aerospace Aluminium Alloys. Surf Eng. 1st ed. Springer, Dordrecht; 1990. p. 260–269.

[73] Zhu L, Xue X-Y, Tang B, et al. Influence of surface plastic deformation on diffusion bonding of high Nb containing TiAl alloy. 2nd Annu Int Conf Adv Mater Eng (AME 2016). Wuhan, China; 2016. p. 635–643.

[74] Barta IM. Low temperature diffusion bonding of aluminium alloys. Weld J Res Suppl. 1964;43:241s–247s.

[75] Zeer GM, Zelenkova EG, Koroleva YP, et al. Diffusion bonding through interlayers. Weld Int. 2013;27:638–643.

[76] Yeh MS, Chuang TH. Low-pressure diffusion bonding of sae 316 stainless steel by inserting a superplastic interlayer. Scr Metall Mater. 1995;33:1277–1281.

[77] Xie R-J, Mitomo M, Zhan G-D. Diffusion Bonding of Silicon Nitride Using a Superplastic β-SiAlON Interlayer. J Am Ceram Soc. 2001;84:471–473.

[78] Ramsey KJ. Method for Diffusion Bonding Aluminium, US Patent. United States; 1990. p. 1–7.

[79] Cook GO, Sorensen CD. Overview of transient liquid phase and partial transient liquid phase bonding. J Mater Sci. 2011;46:5305–5323.

[80] Salazar JMG De, Mcndez FJ, Urena A, et al. Transient liquid phase (TLP) diffusion bonding of a copper based shape memory alloy using silver as interlayer. Scr Mater. 1997;37:861–867.

[81] Habisch S, Peter S, Grund T, et al. The Effect of Interlayer Materials on the Joint and Magnesium. Metals (Basel). 2018;8:1–12.

[82] Dunford D V, Partridge PG. Transient liquid phase diffusion bonding of 8090 AI-Li alloy using copper interlayer. Mater Sci Technol. 1998;14:422–428.

[83] Nami H, Halvaee A, Adgi H, et al. Investigation on microstructure and mechanical properties of diffusion bonded Al / Mg 2 Si metal matrix composite using copper interlayer. J Mater Process Technol [Internet]. 2010;210:1282–1289. Available from: http://dx.doi.org/10.1016/j.jmatprotec.2010.03.015.

[84] Wu F, Chen W, Zhao B, et al. Diffusion Bonding of 1420 Al – Li Alloy Assisted by Pure Aluminum Foil as Interlayer. Materials (Basel). 2020;13:1–12.

[85] Zhang J, Luo G, Wang Y, et al. An investigation on diffusion bonding of aluminum and magnesium using a Ni interlayer. Mater Lett [Internet]. 2012;83:189–191. Available from: http://dx.doi.org/10.1016/j.matlet.2012.06.014.

[86] Assadi H, Shirzadi AA, Wallach ER. Transient liquid phase diffusion bonding under a temperature gradient: modelling of the interface morphology. Acta mater [Internet]. 2001;49:31–39. Available from: www.elsevier.com/locate/actamat.

[87] Tashkandi MA. Friction stir welding and processing. Mater Sci Eng R 50. 2005;50:1–78.

[88] Hwang YM, Lin CH. Friction Stir Welding of Dissimilar Metal Sheets. Steel Res Int. 2010;81:1076–1079.

[89] Threadgill PL, Leonard AJ, Shercliff HR, et al. Friction stir welding of aluminium alloys. Int Mater Rev. 2009;54:49–93.

[90] Yadav D, Bauri R. Effect of friction stir processing on microstructure and mechanical properties of aluminium. Mater Sci Eng A [Internet]. 2012;539:85–92. Available from: http://dx.doi.org/10.1016/j.msea.2012.01.055.

[91] Patel V, De Backer J, Hindsefelt H, et al. High-speed friction stir welding in light weight battery trays for the EV industry. Sci Technol Weld Join [Internet]. 2022 [cited 2022 Mar 4];1–6. Available from: https://www.tandfonline.com/doi/full/10.1080/13621718.2022.2045121.

[92] Reisgen U, Schiebahn A, Sharma R, et al. A method for evaluating dynamic viscosity of alloys during friction stir welding. J Adv Join Process [Internet]. 2020;1:100002. Available from: https://doi.org/10.1016/j.jajp.2019.100002.

[93] El Rayes MM, Soliman MS, Abbas AT, et al. Effect of Feed Rate in FSW on the Mechanical and Microstructural Properties of AA5754 Joints. Adv Mater Sci Eng. 2019;2019:12.

[94] Tashkandi MA. Lap Joints of 6061 Al Alloys by Friction Stir Welding. IOP Conf Ser Mater Sci Eng. Institute of Physics Publishing; 2017.

[95] Ojo OO, Taban E, Kaluc E. Friction stir spot welding of aluminum alloys: A recent review. Mater Test. 2015;57:595–627.

[96] Shahani A, Farrahi A. Effect of stirring time on the mechanical behavior of friction stir spot weld of Al 6061-T6 lap-shear configuration. Proc Inst Mech Eng Part C J Mech Eng Sci. 2019;233:3583–3591.

[97] Refil Friction Stir Spot Welding [Internet]. [cited 2022 Feb 20]. Available from: https://www.twi-global.com/technical-knowledge/job-knowledge/refill-friction-stir-spot-welding-150.

[98] Sato YS, Yamashita F, Sugiura Y, et al. FIB-assisted TEM study of an oxide array in the root of a friction stir welded aluminium alloy. Scr Mater. 2004;50:365–369.

[99] Duong HD, Okazaki M, Tran TH. Effect of welding parameters on mechanical properties of friction stir welded T-lap dissimilar metal joints between 7075 and 5083 aluminum alloys. Mech Eng J. 2019;6:19-91-19–00091.

[100] Zhou C, Yang X, Luan G. Effect of kissing bond on fatigue behavior of friction stir welds on Al 5083 alloy. J Mater Sci. 2006;41:2771–2777.

[101] Balos S, Sidjanin L, Dramicanin M, et al. FSW welding of Al-Mg alloy plates with increased edge roughness using square pin tools of various shoulder geometries. Mater Tehnol. 2016;50:387–394.

[102] Badarinarayan H, Yang Q, Zhu S. Effect of tool geometry on static strength of friction stir spot-welded aluminum alloy. Int J Mach Tools Manuf. 2009;49:142–148.

[103] Badarinarayan H, Shi Y, Li X, et al. Effect of tool geometry on hook formation and static strength of friction stir spot welded aluminum 5754-O sheets. Int J Mach Tools Manuf [Internet]. 2009;49:814–823. Available from: http://dx.doi.org/10.1016/j.ijmachtools.2009.06.001.

[104] Zhang Z, Yang X, Zhang J, et al. Effect of welding parameters on microstructure and mechanical properties of friction stir spot welded 5052 aluminum alloy. Mater Des [Internet]. 2011;32:4461–4470. Available from: http://dx.doi.org/10.1016/j.matdes.2011.03.058.

[105] Yang Q, Mironov S, Sato YS, et al. Material flow during friction stir spot welding. Mater Sci Eng A. 2010;527:4389–4398.

[106] Chu Q, Yang XW, Li WY, et al. Impact of surface state in probeless friction stir spot welding of an Al – Li alloy. Sci Technol Weld Join ISSN [Internet]. 2019;24:200–208. Available from: https://doi.org/10.1080/13621718.2018.1517966.

[107] Suryanarayanan R, Sridhar VG. Process parameter optimisation in pinless friction stir spot welding of dissimilar aluminium alloys using Multi-start algorithm. Proc Inst Mech Eng Part C J Mech Eng Sci. 2020;234:4101–4115.

[108] Bakavos D, Chen Y, Babout L, et al. Material interactions in a novel pinless tool approach to friction stir spot welding thin aluminum sheet. Metall Mater Trans A Phys Metall Mater Sci. 2011;42:1266–1282.

[109] Venukumar S, Muthukumaran S, Yalagi SG, et al. Failure modes and fatigue behavior of conventional and refilled friction stir spot welds in AA 6061-T6 sheets. Int J Fatigue [Internet]. 2014;61:93–100. Available from: http://dx.doi.org/10.1016/j.ijfatigue.2013.12.009.

[110] Xu Z, Li Z, Ji S, et al. Refill friction stir spot welding of 5083-O aluminum alloy. J Mater Sci Technol [Internet]. 2018;34:878–885. Available from: http://dx.doi.org/10.1016/j.jmst.2017.02.011.

[111] Ji S, Li Z, Wang Y, et al. Material flow behavior of refill friction stir spot welded LY12 aluminum alloy. High Temp Mater Process. 2017;36:495–504.

[112] Li G, Zhou L, Luo L, et al. Microstructural evolution and mechanical properties of refill friction stir spot welded alclad 2A12-T4 aluminum alloy. J Mater Res Technol. 2019;8:4115–

4129.

[113] Zhang ZK, Yu Y, Zhang JF, et al. Corrosion behavior of keyhole-free friction stir spot welded joints of dissimilar 6082 aluminum alloy and DP600 galvanized Steel in 3.5% NaCl solution. Metals (Basel). 2017;7.

[114] Uematsu Y, Tokaji K, Tozaki Y, et al. Effect of re-filling probe hole on tensile failure and fatigue behaviour of friction stir spot welded joints in Al-Mg-Si alloy. Int J Fatigue. 2008;30:1956–1966.

[115] Li G, Zhou L, Luo L, et al. Microstructural evolution and mechanical properties of refill friction stir spot welded alclad 2A12-T4 aluminum alloy. J Mater Res Technol [Internet]. 2019;8:4115–4129. Available from: https://doi.org/10.1016/j.jmrt.2019.07.021.

[116] Reilly A, Shercliff H, Chen Y, et al. Modelling and visualisation of material flow in friction stir spot welding. J Mater Process Technol [Internet]. 2015;225:473–484. Available from: http://dx.doi.org/10.1016/j.jmatprotec.2015.06.021.

[117] Farmanbar N, Mousavizade SM, Elsa M, et al. AA5052 sheets welded by protrusion friction stir spot welding: High mechanical performance with considering sheets thickness at low dwelling time and tool rotation speed. Proc Inst Mech Eng Part C J Mech Eng Sci. 2019;0:1–12.

[118] Tier MD, Rosendo TS, Dos Santos JF, et al. The influence of refill FSSW parameters on the microstructure and shear strength of 5042 aluminium welds. J Mater Process Technol [Internet]. 2013;213:997–1005. Available from: http://dx.doi.org/10.1016/j.jmatprotec.2012.12.009.

[119] Freeney TA, Sharma SR, Mishra RS. Effect of welding parameters on properties of 5052 Al friction stir spot welds. SAE Tech Pap. 2006;

[120] Bozzi S, Helbert-Etter AL, Baudin T, et al. Influence of FSSW parameters on fracture mechanisms of 5182 aluminium welds. J Mater Process Technol. 2010;210:1429–1435.

[121] Mahmoud TS, Khalifa TA. Microstructural and mechanical characteristics of aluminum alloy AA5754 friction stir spot welds. J Mater Eng Perform. 2014;23:898–905.

[122] Hornak J, Trnka P, Kadlec P. Magnesium Oxide Nanoparticles : Dielectric Properties , Surface Functionalization and Improvement of Epoxy-Based Composites Insulating Properties. Nanomaterials. 2018;8:1–17.

[123] Neppiras EA. Ultrasonic welding of metals. Ultrasonics. 1965;3:128–135.

[124] Annoni M, Carboni M. Ultrasonic metal welding of AA 6022-T4 lap joints: Part I - Technological characterisation and static mechanical behaviour. Sci Technol Weld Join. 2011;16:107–115.

[125] Carboni M, Annoni M. Ultrasonic metal welding of AA 6022-T4 lap joints: Part II - Fatigue behaviour, failure analysis and modelling. Sci Technol Weld Join. 2011;16:116–125.

[126] Bergmann JP, Köhler T, Pöthig P. Ultrasonic welding. Adv Join Process [Internet]. 2021 [cited 2022 Mar 4];239–267. Available from: https://linkinghub.elsevier.com/retrieve/pii/B9780128207871000073.

[127] Ni ZL, Ye FX. Ultrasonic spot welding of aluminum alloys: A review. J Manuf Process. 2018;35:580–594.

[128] Ni ZL, Yang JJ, Hao YX, et al. Ultrasonic spot welding of aluminum to copper: a review. Int J Adv Manuf Technol. 2020;107:585–606.

[129] Mohammed SMAK, Dash SS, Jiang XQ, et al. Ultrasonic spot welding of 5182 aluminum alloy : Evolution of microstructure and mechanical properties. Mater Sci Eng A.

2019;756:417–429.

[130] Siddiq A, Ghassemieh E. Thermomechanical analyses of ultrasonic welding process using thermal and acoustic softening effects. Mech Mater. 2008;40:982–1000.

[131] Kong CY, Soar RC, Dickens PM. A model for weld strength in ultrasonically consolidated components. Proc Inst Mech Eng Part C J Mech Eng Sci. 2005;219:83–91.

[132] Chen KK, Zhang YS, Wang HZ. Study of plastic deformation and interface friction process for ultrasonic welding. Sci Technol Weld Join. 2017;22:208–216.

[133] Li H, Cao B. Effects of welding pressure on high-power ultrasonic spot welding of Cu / Al dissimilar metals. J Manuf Process. 2019;46:194–203.

[134] Kong CY, Soar RC, Dickens PM. Characterisation of aluminium alloy 6061 for the ultrasonic consolidation process. Mater Sci Eng A. 2003;363:99–106.

[135] Kong CY, Soar RC, Dickens PM. Optimum process parameters for ultrasonic consolidation of 3003 aluminium. J Mater Process Technol. 2004;146:181–187.

[136] Watanabe T, Yanagisawa A, Konuma S, et al. Effect of oxide film on bond strength of ultrasonically welded joints, and welding process. Study of ultrasonic welding of dissimilar metals (2nd Report). Weld Int. 1999;13:936–944.

[137] Fujii HT, Endo H, Sato YS, et al. Interfacial microstructure evolution and weld formation during ultrasonic welding of Al alloy to Cu. Mater Charact. 2018;139:233–240.

[138] Matsuoka S ichi, Imai H. Direct welding of different metals used ultrasonic vibration. J Mater Process Technol. 2009;209:954–960.

[139] Macwan A, Kumar A, Chen DL. Ultrasonic spot welded 6111-T4 aluminum alloy to galvanized high-strength low-alloy steel: Microstructure and mechanical properties. Mater Des [Internet]. 2017;113:284–296. Available from: http://dx.doi.org/10.1016/j.matdes.2016.10.025.

[140] Zhang G, Takahashi Y, Heng Z, et al. Ultrasonic weldability of al ribbon to cu sheet and the dissimilar joint formation mode. Mater Trans. 2015;56:1842–1851.

[141] Gester A, Wagner G, Pöthig P, et al. Analysis of the oscillation behavior during ultrasonic welding of EN AW-1070 wire strands and EN CW004A terminals. Weld World [Internet]. 2022;567–576. Available from: https://doi.org/10.1007/s40194-021-01222-z.

List of figures

bonding within the region I at indicated locations; (b1) and (b2) partial and complete metallurgical bonding in region II at indicated locations [102].

Figure 10. Comparative plots of maximum and minimum tensile shear forces of welding samples by different types of FSSW and different aluminium alloys from 5xxx series (PLT-FSSW – pinless tool friction stir spot welding; CFSSW – conventional FSSW; WFSSW - walking FSSW; PFSSW – protrusion FSSW; FFSSW – flat FSSW; RFSSW – Refill FSSW) [5,31,103,110,117–121].

Figure 11. Scanning transmission electron macrographs of weld faying interface: (a) bright field of sample welded with low heat input – 1000 rpm (lower magnification); (b) annular dark-field image of (a) (higher magnification); (c) bright field of sample welded with high heat input – 4500 rpm (lower magnification); d high-angle annular dark-field image of (c) (higher magnification) [5].

Figure 12. Scanning electron images of aluminium alloy (AA 6061) specimen obtained with ultrasonic consolidation process (a) an unclean specimen showing ~500 nm thick oxide film along with weld interface. Insert shows magnification of the residual oxide layer (b) weld interface with contact area and oxides dispersed along with the interface [134].

Figure 13. Scanning electron microscope images at the weld interface of ultrasonic welded Al/Cu specimen with elemental maps of the area presented in SEM image obtained with Energy-dispersive X-ray spectroscopy (adapted from [137]).Matsuoka et al. [138] had a similar observation during the study of ultrasonic welding of aluminium-copper joints. With welding parameters, it is possible to disperse the residual oxide layer within the weld zone which allows metal-to-metal contact and atomic diffusion to occur.